A

Dissertation Report

On

Heat and Mass Balance Study of a Single Slope Solar Still

Submitted in Partial Fulfillment of the Requirements for the Award of Degree of

Master of Technology

In

Thermal Engineering

By

ANKUR AGRAWAL

2015PTE5169

Under the supervision of

Dr. NIRUPAM ROHATGI

Associate Professor

Department of Mechanical Engineering

M.N.I.T. Jaipur, India

DEPARTMENT OF MECHANICAL ENGINEERING

MALAVIYA NATIONAL INSTITUTE OF TECHNOLOGY,

JAIPUR

JUNE 2017

DEPARTMENT OF MECHANICAL ENGINEERING
JAIPUR (RAJASTHAN)-302017
MALAVIYA NATIONAL INSTITUTE OF TECHNOLOGY

CERTIFICATE

This is certified that the dissertation report entitled **"Heat and Mass Balance Study of a Single Slope Solar Still"** prepared by **Ankur Agrawal** (ID-2015PTE5169), in the partial fulfillment of the award of the Degree **Master of Technology** in **Thermal Engineering** of Malaviya National Institute of Technology Jaipur is a record of bonafide research work carried out by him under my supervision and is hereby approved for submission. The contents of this dissertation work, in full or in parts, have not been submitted to any other Institute or University for the award of any degree or diploma.

Date:

Dr. NIRUPAM ROHATGI
Associate Professor
Department of Mechanical Engineering
MNIT, Jaipur, India

Place:

DEPARTMENT OF MECHANICAL ENGINEERING
MALAVIYA NATIONAL INSTITUTE OF TECHNOLOGY
JAIPUR (RAJASTHAN)-302017

DECLARATION

I **Ankur Agrawal** hereby declare that the dissertation entitled **"Heat and Mass Balance Study of a Single Slope Solar Still"** being submitted by me in partial fulfillment of the degree of **Master of Technology** in **Thermal Engineering** is a research work carried out by me under the supervision of **Dr. Nirupam Rohatgi,** and the contents of this dissertation work, in full or in parts, have not been submitted to any other Institute or University for the award of any degree or diploma. I also certify that no part of this dissertation work has been copied or borrowed from anyone else. In case any type of plagiarism is found out, I will be solely and completely responsible for it.

Date:

Place:

Ankur Agrawal
Master of Technology
Thermal Engineering
(2015PTE5169)

ACKNOWLEDGEMENT

I feel an immense pleasure to express my sincere gratitude to my supervisor **Dr. Nirupam Rohatgi**, Department of Mechanical Engineering, for his constant encouragement and guidance from inception to completion of this dissertation work by taking interest and giving personal attention to the same. His valuable feedback, criticism and moral support have been a great source of inspiration for broadening my horizons in this area of research. In this respect, I feel myself lucky to have him as my supervisor.

I would like to express my deepest gratitude to **Prof. Jyotirmay Mathur**, **Prof. Dilip Sharma**, **Dr. G.D. Aggarwal** and **Prof. S.L. Soni**, Department of Mechanical Engineering, Malaviya National Institute of Technology Jaipur, for their valuable guidance and support throughout my project work.

I am extremely thankful to **Prof. G. S. Dangayach**, Head, Department of Mechanical Engineering, MNIT, Jaipur and all the faculty members for their motivation and moral support.

I feel indebted to **Gautam Saini**, **Karan Yadav**, **Chandra Sekhar**, **Ankit Goyal**, **Mitesh Varshney**, **Paras Gandhi** and all my **colleagues** for their constant help and moral support throughout my dissertation work. I also express my deepest gratitude to **my parents** for their blessings and affection, without which I would not be able to endure hard time and carry on with my studies.

(Ankur Agrawal)

ABSTRACT

Water is an essential requirement to sustain life. Although water is a renewable resource, yet most of the water present on earth is not suitable for direct usage. The world's supply of drinkable water is steadily decreasing, with depletion occurring most prominently due to rising population, Urbanization, Industrialization and environmental pollution. One-third of the world's population live in countries with insufficient freshwater supply. Natural resources of water can only meet the fresh water demand up to the limited extent. In order to meet the ever-increasing demand of potable water, purification of saline water with the help of effective water desalination method becomes necessary.

Solar still is a device which works on solar desalination method. It can solve the problem of potable water without using the high-grade energy. It is potentially applicable to provide fresh water for remote areas where electrical energy is rather scarce. Solar still suffers greatly with the problem of its low productivity of drinkable water. It is required to improve its productivity. Therefore, in this study heat and mass of the single slope solar still is analyzed to find and propose the areas which can be improved to enhance the performance of solar still.

In this work, heat and mass balance of the single slope solar still has been done. A single slope solar still is made up of galvanized iron sheet of 24 gauge, and having the basin area 0.8 m^2. A transparent glass of 5 mm thickness, of 1m^2 surface area used as glass cover which is inclined at 26.8° angle with the horizontal plane. In order to have heat and mass balance of solar still several experiments have been carried out in month of March 2017 under the climatic condition of MNIT Jaipur. These experiments are carried out with the variation in feed water quantity, i.e. 10L, 15L, and 20L. On the basis of clear sky or minimal variation in solar intensity, six set of the experimental data are selected, two experimental data for 10L, 15L, and 20L each. The objective of this study is to determine how much energy is coming through the glass cover as an input to the solar still, how much energy is utilized effectively in producing distilled water and how much of energy is lost in different forms from the solar still.

On the basis of experimental analysis, several results are observed firstly, 9 – 10% of total energy that falls on the surface of the glass throughout a day is reflected by the glass cover which various with the angle of incident solar radiation. Secondly, 3% of total energy lost in the form vapour leakage. Thirdly, 2 – 3% of energy lost with produced distilled water which containing some heat within. Fourthly, vapour loses increase with the increase in the average temperature of the water in basin during daylight. There is also some amount of unaccounted energy which is due to the experimental limitation.

Table of Contents

List of Figures

List of Tables

Nomenclature

A	Surface area [m^2]
A_s	Surface area of side walls [m^2]
Gr	Grashof no.
g	acceleration due to gravity [m/s^2]
h	Heat transfer coefficient [W/m^2 K]
h_{fg}	enthalpy of evaporation [J/kg]
I(t)	solar radiation on inclined surface [W/m^2]
k	Thermal conductivity of air [W/m K]
L_c	characteristic length [m]
M	total mass [kg]
m	mass [kg]
Nu	Nusselt number [hD_h/k]
Pr	Prandtl number [$\mu C_p/k$]
Q	Heat transfer [kJ]
T	Temperature [°C]
V	wind velocity [m/s]

Greek symbol

ε	emissivity
β	volumetric expansion coefficient, /K
ν	kinematic viscosity, m^2/s

σ	Stefan boltzmann constant, 5.67 W/m^2K^4
ρ	Density of air [kg/m^3]

Abbreviations

CFD	Computational Fluid Dynamics
EPA	Environmental Protection Agency
GI	Galvanized Iron-sheet
TDS	Total Dissolved Solid
MSF	Multi-Stage Flash Distillation
MED	Multiple Effect Distillation
SS	Solar Still
VCE	Vapour Compression Evaporation
UNEP	United Nations Environment Programme
UV	Ultra-Violet rays

Subscripts

a	Air
abm	Ambient
bck	Back Surface
btm	Bottom Surface
evp	Evaporation
c	Convective Mode of Heat Transfer
g	Glass Surface
inner	Inner Surface of Glass Cover
r	Radiation Mode of Heat Transfer
v	Vapor
L, ls	Left Surface
outer	Outer Surface of Glass Cover
R, rs	Right Surface
ref	Reflection
mw	Distilled Water
vl	Vapor Loss
un	Unaccounted
wb	Basin Water

Chapter 1.
Introduction

1.1. Availability of Water – World Scenario

Water is the necessity of human along with food and air. It plays an important role in the development of a country. Around 71% part of the Earth is covered with water, out of which 96.5% of the earth's water is found in oceans, and remaining 3.5% in groundwater, glaciers and the polar ice. Only 2.5% of the earth's water is fresh water and 98.8% of that fresh water is ground water and ice. Less than 1% of freshwater is within the human reach. But the access of potable water is narrowing with the time due to increasing in population.

The world's water consumption rate is doubling every 20 years. The United Nations Environment Programme (UNEP) stated that one-third of world's population lives in areas with insufficient freshwater. Almost one-fifth of the world's population lives in countries where water is scarce. By the year 2025, fresh water demand will exceed the supply by 56% due to persistent regional droughts, shift in the population to the cities and increase in pollution of water. As a result of this two-third of world's population will not be having fresh water even for their house-hold, by 2025.

1.2. Availability of Water - Indian Scenario

The geographical area of India is about 329 million hectares (2.45% of the earth's land mass) and its population is 1210 million based on the 2011 census, which is about 17% of that of the world. The renewable fresh water resources of the country are 1,869 km^3/year, which are only about 4% of that of the world and is insufficient to fulfil the need of such a vast population. More than 100 million people in India are living in places where water is severely polluted. Out of the 632 districts only 59 districts were found safe for drinking water, after examining the quality of ground water.

Water usage is increasing everywhere. Currently, on a global basis, 69% of all water withdrawn for human use on annual basis is soaked up by agriculture (mostly in the form of irrigation), industry accounts for another 23% of the total available water and domestic use (household, drinking water, sanitation) accounts for about 8%. These global averages vary a great deal between regions. In India, it is estimated that sectoral

water requirements by 2010 were 85%, 7%, 5% and 3% for agriculture, domestic, industries and energy, respectively. (Water Resources Scenario of India, 2007)

The annual precipitation including rainfall in India is about 4,000 km^3 and average potential flow in the rivers is about 1,869 km^3 while the rest is lost in evaporation, flows into sea during the floods and partly contributes to groundwater reservoirs following the complex hydrological cycle.

1.3. Desalination Technologies

Desalination is a process that extracts salt contains from saline water. A desalination process essentially separates saline water into two parts - one that has a low concentration of salt (treated water or product water), and the other with a much higher concentration than the original feed water, usually referred to as brine concentrate or simply as ‘concentrate

The water desalination processes can be divided mainly into two types, i.e. membrane processes and thermal processes, as shown in Fig. 1.1.

The other alternative technologies are freezing and ion exchange which are not widely used. They are operated by conventional or renewable energy sources to produce potable water.

1.3.1. Membrane Desalination

Membrane process involves passage of water through a semipermeable membrane under pressure. The pressurization reverses the spontaneous transport of water that would occur from the dilute to the more concentrated side to equalize the free energy of the fluids. The most common membrane desalination processes are:

i. Reverse Osmosis (RO)
ii. Electro-Dialysis (ED)
iii. Membrane Distillation (MD)

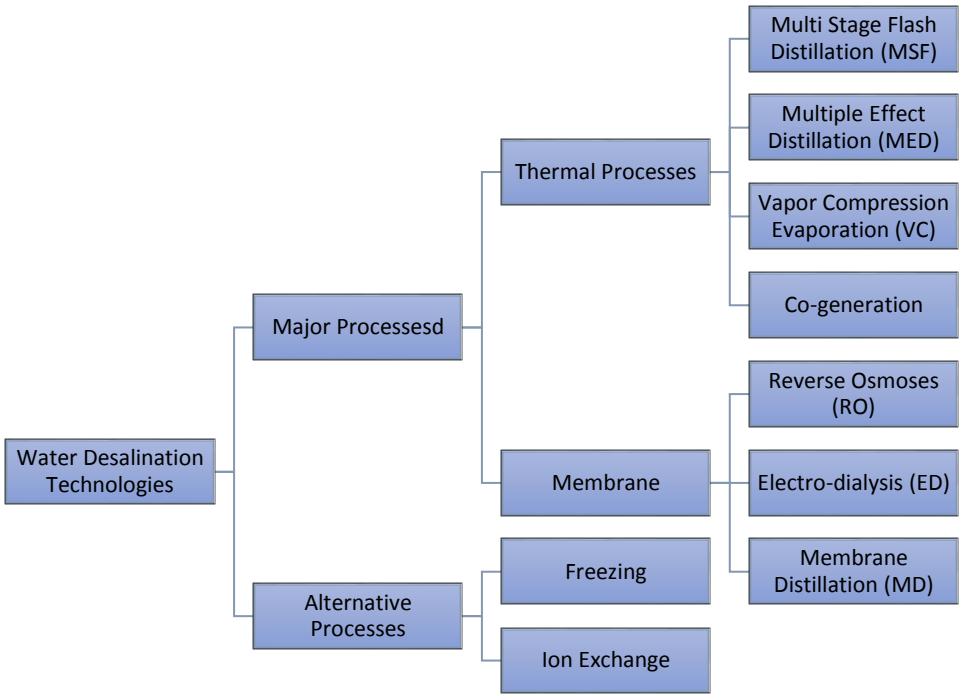

Figure 1.1: Water Desalination Technologies

1.3.2. Thermal Desalination

The thermal process is a multistep distillation process that ranges from simple small-scale distillation to commercial sea-water desalination. Although its energy consumption and costs are generally higher than membrane processes but it provides most of the processed drinking and process water.

The most common thermal desalination methods are:

- Multi stage flash distillation (MSF)
- Vapour compression (VC)
- Solar Water desalination

1.3.3. Other Desalination Process

Many number of other process have been used to convert saline water to potable water. Most of the process have not achieved the level of commercial success that reverse osmosis (RO) and distillation had. These are:

i. Freezing Desalination Process

ii. Ion Exchange Desalination Process

1.4. Solar Stills:

Solar still is the solar device which takes input as the solar radiation from the Sun and converts brackish water to potable water. Solar stills output mainly depends on the amount of solar radiation receiving from the Sun. The areas lying between 35˚ N to 35˚ S latitudes receive maximum solar radiation. India (8˚ N to 35˚ N) is blessed with large amount of solar radiation and therefore quite suitable for use of solar still .

Two types of solar stills are passive solar still and active solar still. Classification of solar stills is shown in Fig 1.2.

1.4.1. Passive Solar Stills

In this type of Solar still, there is no other source of energy except the solar energy and the rise in basin water temperature is due to solar radiations only.

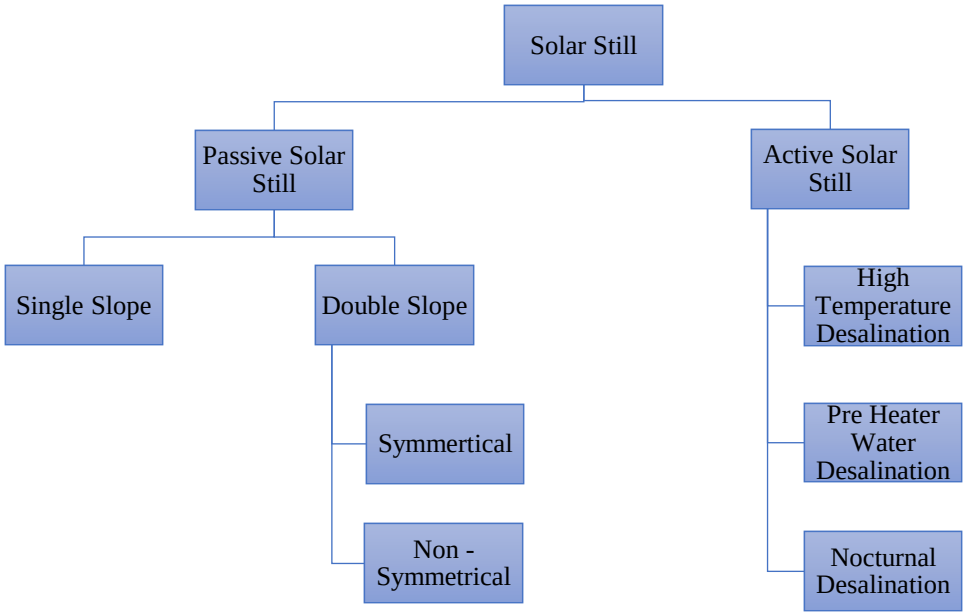

Figure 1.2: Classification of Solar Stills

I. Single Slope Passive Solar Still

Single slope solar still consists of a water basin and a glass cover at the top. Raw water is fed in the basin. The solar radiations enter the solar still, heat the water in the basin which evaporates as pure vapours and condenses at the inner surface of the glass. The

water droplets that form at the underside of the glass slide down the glass due to gravity effect and collect on the tray attached to the bottom of the glass.

II. Double Slope Passive Solar Still

Double slope solar still consists of the two-storey water basin and raw water is fed in both the basins. The solar radiations enter both the basins as the top basin bottom is made of glass, heat the water in basins which evaporates as pure vapours and condensed at the underside of the both the glasses. The water droplets that form at the underside of the glasses slide down the glass due to gravity effect and collected on the tray attached to the bottoms of the glasses.

1.4.2. Active Solar Stills

In this type of Solar Still, additional heat is given to increase the basin water temperature by coupling it with heat sources like flat plate collector or waste heat heat exchanger to enhance the performance of the solar still. The amount of distillate output increases in an active solar still. Active solar stills can be further divided into three groups as explained below:

I. High-Temperature Desalination Active Solar Still

The flat-plate solar collector is used to heat the raw water, and the hot raw water is fed into solar still for distillation process. The solar collector coupled with solar still increases the productivity of the solar still.

II. Pre-Heated Water Desalination Active Solar Still

This is the technique in which waste hot water from various industries like chemical industry, paper industry, thermal power plants, food-processing industries is utilized in a solar still. The waste hot water gives higher output as it requires less heat to evaporate.

III. Nocturnal Desalination Active Solar Still

Nocturnal desalination is the working of solar still in absence of sunlight. The solar energy is stored in the day time and utilized in the night time, and the waste heat can also be used during night hours. In a conventional solar still, high water depth is taken that is heated in the day time, and a significant amount of heat is stored by water within it, and the stored heat is utilized in the night hours.

1.5. Objective

The objective of the present work is to study the heat and mass balance of a single slope passive solar still and to examine various losses affecting the performance of a solar still. The various heat and mass losses that have been accounted for are:

- Loss of water as vapours from the solar still.
- Loss of solar radiations due to reflection of the incident radiations from of the glass,
- Loss of heat from the side walls of the solar still,
- Loss of heat from the bottom walls of the solar still,
- Loss of heat due to convection from the upper surface of the glass,
- And the heat carried by the distilled water.

1.6. Outline of the thesis

Chapter 1: Introduction

In this chapter availability of potable water, various techniques of water purification, types of solar stills and advantages and disadvantages of SS has been discussed. The objective of the study and the thesis outline have also been stated**.**

Chapter 2: Literature review

Literature review has been subdivided into four sections. Experimental work on solar still forms the first section. In the second section, Solar Stills Coupled with other Energy Consuming Systems have been discussed. In the third section CFD simulation work on solar still has been reviewed. Finally, conclusions from the literature have been discussed and accordingly plan for the present study has been developed.

Chapter 3: Solar Still

In this chapter working principle of Solar Still along with Theoretical Analysis of Internal and External Heat Transfer have been discussed. The equations involved in the Heat and Mass Balance of Solar Still have also been described.

Chapter 4: Experimental Setup

Experimental Setup discusses the components used in the construction of Solar Still. The orientation of the system, the instruments used in the experiments, and Calibration of Thermocouples are also discussed in this chapter.

Chapter 5: Experimentation

The chapter describes experiment procedure, lists observed data and Calculation for Heat and Mass for the solar still.

Chapter 6: Results and discussion

This chapter explains various heat losses, like Energy Lost through Reflection of Solar Radiation, Heat content in Distilled Water and Leakage of water vapors. Heat Balance charts of Solar Still are also shown in this chapter.

Chapter 7: Conclusions

The conclusions based on the study have been discussed in this chapter. Some suggestions for future work have been included at the end of this chapter.

Chapter 2.
Literature Survey

Solar water distillation is an oldest and cost–effective method to provide potable water in remote villages where the electricity is rather scarce. The device that carries out the solar distillation is generally known as the solar still. Solar still has many advantages such as low cost, simple construction, low maintenance, etc. but it has a significant disadvantage of lower efficiency and low productivity of potable water. Various theoretical, experimental and simulation works have been done on the solar stills to improve the performance.

Literature review on solar water distillation has been divided into the following sub-sections:

- Experimental and Theoretical work done on solar still
- Hybrid solar stills
- CFD simulation studies

2.1. Experimental and Theoretical Studies

There were several attempts to improve the design of solar stills and to develop the mathematical models for various types of solar stills. In this section, the research papers on experimental work on the solar still have been discussed.

2.1.1. Use of Reflectors

Kabeel et al. (2013) investigated a modification in Solar Still through internal reflectors. They compared modified stepped solar still with trays and conventional solar still at Kafrelsheikh University, Egypt. In this study, effect of a reflecting mirror on the vertical wall of the steps of stepped still was investigated on the productivity of water. Theoretical as well as experimental investigation was carried out. The results indicate that the productivity of the modified stepped type solar still with and without internal reflectors is higher than that of conventional solar still by 75% and 57% respectively. Also, the efficiency for modified stepped type solar still with and without internal reflectors, and conventional solar still is approx. 56%, 53% and 34% respectively.

Omara et al. (2014) carried out the experimental study on modified stepped type Solar Still and compared its result with the conventional solar still. In a modification of stepped still, mirrors were used as internal and external reflectors to improve the efficiency along with its productivity. Two pieces of mirror were used for the developing external reflector one at the bottom and another was at the top of the glass cover which rested on the inclined frame. The purpose of the external reflector was to increase the incident solar radiation. To evaluate its influence on the performance of the Still under the climatic condition of Kafrelsheikh University, Egypt, a comparative study was carried out over modified stepped solar still and conventional solar still. The results indicate that during the experiment, the productivity of distilled water of the modified stepped type solar still with internal and external reflectors was significantly higher than that of conventional still by 125%.

2.1.2. Use of PCM as Heat Storage Material

Omara et al. (2013) carried out simulation for the solar still using phase change material (PCM) and gave the transient mathematical models of a passive solar still. The function of PCM is to store the thermal energy during the day and release the stored energy during night when surrounding temperature falls. The PCM pockets were placed under the basin liner of the solar still. This study also gives energy balance equations for different components of the solar still as well as for the phase change material. Numerical computations have been carried out for three different PCMs which have different melting temperatures are shown in Table 2.1. The results showed that excess energy produced during the day hours was stored in the PCM which was later released during the night. The result also showed that the distillate output and efficiency of PCM based solar still, increases with increase in the melting points of the PCMs. The efficiency of passive solar still using PCM which has the highest melting temperature (56 °C) is 70%.

El-Sebaii et al. (2009) used PCM below the basin liner of a passive solar still to enhance the performance of the solar still. The effect of the mass of the PCM on the daily productivity and efficiency of the still was investigated. It was found that daytime productivity decreases with increase in the mass of PCM but overnight productivity and daily productivity increases significantly with increase in mass of the PCM due to the increase in the amount of the heat storing capacity of the phase change material. The

best result was obtained with the daily productivity of 9.005 Ltrs/m^2 with an efficiency of 85.3% on a typical summer day (ambient temp. up to 50 °C) with stearic acid of 3.3 cm depth as PCM (52 °C melting temperature), whereas 4.998 Ltrs/m^2 was produced on the same day by the still without the PCM.

Table 2.1: Physical Properties of the Phase Change Materials

PCM Type	Specific heat: solid/liquid C_p (J/kg°C)	Thermal conductivity Solid/liquid K (W/°C m)	Density Solid/liquid ρ (kg/m^3)	Melting temperature T_m (°C)	Latent heat L (kJ/kg)
Paraffin C18	1900/2240	0.376/0.148	814/774	42	242
Paraffin 52-54	2195/2950	0.232/0.150	900/814	52	188
Paraffin wax	2950/2510	0.240/0.240	818/760	56	226

2.1.3. Use of Nanoparticles

Singh et al. (2011) investigated improvement in the performance of a single slope solar still with without the use of nanofluids and compared the same with that of a solar still w/o nano-fluids. Basin of the Solar still was also coated with a black paint. Heat transfer enhancement in the solar still was one of the primary parameter, which led to higher productivity. They found that thermal conductivity of the water used in the solar still increased by 20% and distillation process was faster by 20% than that in the case solar still with normal water. When the overall efficiency of the solar still was evaluated between the ordinary water and nanofluid, there was almost 5% increment in the efficiency of the still using Nanofluids.

Gnanadason et al. (2013) analyzed and compared the performance of a single slope solar still using Nanofluids with the regular water. A single slope solar still was fabricated using an aluminum sheet and tested for both the conditions using with and without Nanofluids. The distilled water production rate of a single slope solar still depends on the design of the solar still, absorbing materials, insulation material, depth of water and salt concentrations inside the still. The aluminum has the higher thermal conductivity which increases the heat transfer rate and yields 6 liters/day output that is higher than that and the efficiency of the single slope solar still made up of GI sheet by

55%. Further, a 205 improvement was found in the efficiency of the solar still using nanofluids.

2.1.4. Use of Fins in Basin

Appadurai et al. (2015) integrated solar still with a fin type solar pond to enhance the productivity of the solar still and also presented a theoretical and experimental analysis of a conventional solar still, fin type solar still and fin type solar still integrated with fin type solar pond. The experimental work was carried out at the site of Tirunelveli which had the latitude of 10°. The addition of the fins in a solar still was a plus point in improving the thermal efficiency of the single basin solar still by increasing the overall productivity of distilled water over 24 hrs. When fins were integrated at the basin, the heat transfer rate from basin to water was increased. Results for fin type solar still, conventional solar still integrated with fin type solar pond and fin type solar still integrated with a fin type solar pond show increase in the distilled water collection, by 45.5%, 47%, and 50%, respectively.

Srithar et al. (2016) have integrated square and circular fins in the basin of solar still and carried out experimental and theoretical analysis for its performance. A mild steel square hollow pipe (0.019 m side length × 0.07 m height) and circular pipe (0.03 m diameter × 0.07 m height) were used as fins to modify still. The performance of the system was analyzed by varying the depth (1 cm, 2 cm, 3 cm and 4 cm) of water in the basin. The distillate output attains a maximum of 4.55 kg/m^2/day in the still with square fin and covering with a wick, whereas the conventional still yields a maximum of 3.16 kg/m^2/day. In this work, they also calculated the energy payback time which was less than a year for each case and it could be further reduced by increase in operational days of the solar still. Total CO_2 emission mitigation was about 5.6 to 36.6 tons with the lifetime of 5 to 30 years in square fin-integrated still.

2.2. Solar Stills Coupled with other Energy Consuming Systems

There were several attempts to integrate solar stills with other energy systems and to develop the mathematical model for various types of solar stills. In this section, experimental work on solar stills have been discussed.

2.2.1. Integration with Refrigeration Cycle

Abdul-Wahab et al. (2012) carried out an experimental study over the solar still which was integrated with a refrigeration cycle for different water depth and temperature of feed saline water. Experiments were conducted under the meteorological conditions of Muscat, Sultanate of Oman. When the temperature of the feed saline water was 35 °C, it was observed that the daily yield of distilled water obtained were 6670, 4940, and 3930 ml/day with depths of water 8, 6, and 4 cm, respectively. When feed water temperature dropped to 30 °C, it was observed that the daily yield of distilled water obtained was 9500, 10080 and 6400 ml/day for respective water depths of 8, 6, and 4 cm.

2.2.2. Integration with Solar Collector

Badran et al. (2005) integrated Solar Collector with Solar Still and performed the experiment under local conditions of Amman, Jordan. In this, an outlet of the solar flat-plate collector was connected to the inlet of Still such that feed to Still was supplied from the collector instead of a storage tank. They have used two different feed waters, tap water and salt water and compared its effect on the productivity. Three modes of operation were studied: still operating alone for the whole day, still integrated with the solar collector for daylight only, and for still connected to a collector for the whole day. In terms of productivity, the best result was found with tap water in which distilled water production increased by 230% in the cases for Solar Still integrated with Solar collector.

Narayana et al. (2016) integrated flat plate collectors in series with a solar still and its effect on the performance of the solar still was studied. The solar still has basin area of 1 m^2 and glass cover inclination of 30°. Each FPC has an effective area of 2 m^2 was attached with the solar still in series. In this study, experiments were conducted for 24-hrs during the summer months for active solar distillation system. An effective inclination of 5° for flat plate collector was used. The result showed an increment of

41% and 0.47% in productivity and efficiency respectively when the solar still with two FPCs was compared to the solar still with single FPC. When the solar still connected with three FPCs in series, it showed an increment of 89% in productivity and 0.48% increment in efficiency as compared to the solar still with single FPC. The increase in distilled water yield for the still with FPCs in series is due to the high water temperature that was fed to the still.

2.2.3. Integration with Solar Pond

Velmurugan et al. (2009) investigated enhancement in the productivity of the solar still by integrating a mini solar pond with stepped solar still followed by a single slope solar still in series. For further augmentation of the yield, sponges, baffle plate, fins, pebble, and wicks are added. Productivity of this modified the solar stills was studied for the whole day. Efficiency and percentage increase in yield of distilled water for these modifications were also analyzed. In these experiments industrial effluent water was as feed. The maximum increment in the productivity was found to be 80% when sponge and fin were used in the both stepped type solar still and single slope solar still.

2.3. Simulation Studies

Vyskocil et al. (2014) used a condensation model in commercial CFD-Fluent. The condensation model developed for the transport model in Fluent, and it was suitable for compressible as well as an incompressible flow of the mixture (air-steam) with additional non-condensable gas. The condensation model in Fluent consists of two parts – condensation on the wall and condensation in volume. Condensation on the wall was evaluated from diffusion of steam through a layer of non-condensable gasses near the wall whereas, condensation in volume was modeled by returning to saturation in constant time scale" method.

Rahbar et al. (2015) performed 2-D CFD simulation to enhance the performance of a solar still for a given cost. In this study, they investigated the ability of a 2-D CFD simulation of tubular solar still for the computation of heat and mass transfer within it. The results of CFD simulation showed good agreement with the experimental data reported in the literature. This paper also estimated relationship for heat and mass transfer coefficient, and water productivity for the tubular solar still. Based on these

relationships, a characteristic curve was given showing a direct effect of water temperature and the inverse effect of glass temperature on the performance of a tubular solar still.

Rahimi et al. (2011) developed a CFD based two-phase three-dimensional model of solar still in ANSYS-CFX. In this work, volume of fluid (VOF) model was used for modeling the two-phase liquid, water and a mixture of air and water vapor. No turbulence model was used as the water was taken as stagnant and vaporization rate was low. In this work, simulation results were compared with already available experimental results. Simulated data on the temperature of water, the temperature of vapor along with the heat transfer coefficient had good agreement with the experimental data.

2.4. Conclusion from Literature Review

Following are the observations on the basis of literature study:

- Productivity rate depends on the temperature difference between the glass cover and water basin temperature, more the temperature difference more the productivity rate.
- Total productivity of the distilled water for a whole day decreases with the increase in the feed water quantity, this is due to increase in the amount of heat that required to raise the temperature of the basin water or low temperatures achieved for higher feed water quantity.
- The yield of distilled water is increased by flowing water film over the upper surface of the glass cover of the multi-basin still. This is because of the fall in temperature of the glass cover as its heat gets transferred to the water film which leads to faster rate of the condensation of the water vapour on the glass cover.
- Providing additional area for condensation increases the condensation rate as well as the productivity of the distilled water.
- Using PCM, the productivity increases as it stores a reasonable amount of thermal energy and after sunset PCM acts as a heat source for the basin and the temperature of the glass cover is much cooler than that in the daytime. This develops more temperature difference between the glass cover and basin water which helps in increase in the productivity.

- The flat plate collector should be disconnected during off-sunshine hours to reduce the heat loss through the collector.

Chapter 3.
Solar Still

3.1. Working Principle of Solar Still

Solar still is an air tight basin, usually constructed out of galvanized iron sheet (GI-sheet) with a top cover having transparent material like Glass or plastic sheet. Generally, the inner surface of solar still is blackened for absorbing solar radiation efficiently. There is a collecting tray to collect the distillate output. The saline water is fed into the basin through an inlet and the fresh water is collected in a vessel placed at the outlet, as shown in Fig. 3.1.

The basic principle of solar still is similar to hydrological cycle of evaporation and condensation. After reflection and absorption by the glass cover, the remaining solar radiation is transmitted inside the airtight basin where part of it is reflected by the water surface, another part of it is absorbed by the water and the remaining part of the solar radiations transmitted though the water is absorbed by the blackened surface. After the saline water gets heated up and starts evaporating. Salt and microbes which are present in the water are left behind in the water. The evaporated water gets condensed on the inner surface of the glass cover after releasing the latent heat. The condensed water trickles down due to gravity in the collecting channel provided at lower end of the glass cover and it is taken out from the system for further use.

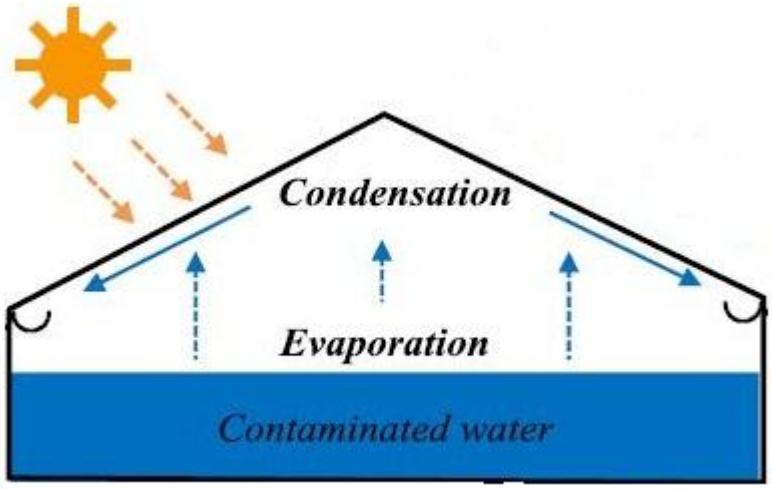

Figure 3.1: Working Principle of Solar Still

3.2. Analysis of the Heat Transfer

The heat transfer in solar still system can be classified in terms of external and internal modes. The external heat transfer mode is primary governed by conduction, convection and radiation. These heat transfer are from the glass cover, bottom and side surfaces of the solar still. Heat transfer within the solar still is by evaporation, convection and radiation. In this case convective heat transfer occurs simultaneously with evaporative heat transfer and these two heat transfer processes are independent of radiative heat transfer as shown in Fig. 3.2

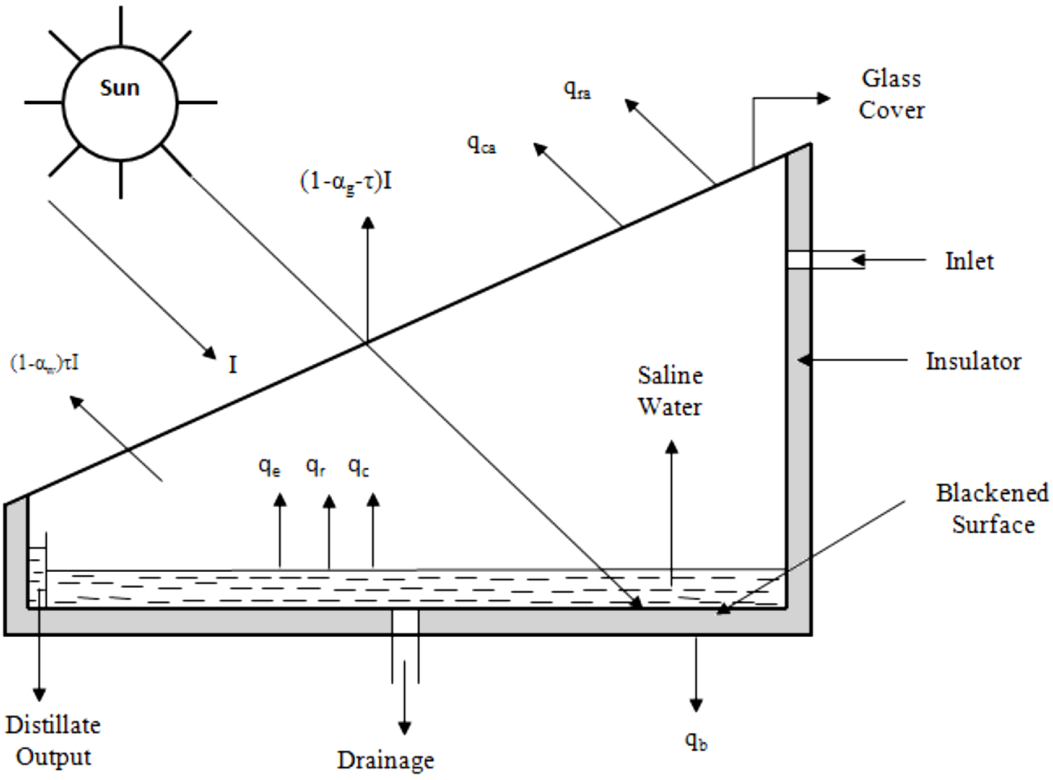

Figure 3.2: Schematic Diagram of Heat Flow

3.2.1. External Heat Transfer

Heat transfer out of the solar still through glass cover is called top loss. It is mainly due to convection (natural as well as forced) and radiation loss from the glass cover to the ambient. It can be expressed as;

$$\dot{Q}_{g-a} = \dot{Q}_{r,g-a} + \dot{Q}_{c,g-a} \tag{3.1}$$

where,

$$\dot{Q}_{r,g-a} = \varepsilon_g A_g \sigma[(\mathrm{T_g}+273)^4 + (\mathrm{T_{amb}}+273)^4)] \quad (3.1.1)$$

$$\dot{Q}_{r,g-a} = h_{rg}(\mathrm{T_g} - \mathrm{T_{amb}}) \quad (3.1.2)$$

$$h_{rg} = \frac{\varepsilon_g A_g \sigma[(\mathrm{T_g}+273)^4 + (\mathrm{T_{amb}}+273)^4)]}{(\mathrm{T_g} - \mathrm{T_{amb}})} \quad (3.1.3)$$

And,

$$\dot{Q}_{\mathrm{c},g-a} = h_{cg}\,\mathrm{A_g}(\mathrm{T_g} - \mathrm{T_{amb}}) \quad (3.1.4)$$

Substituting the expression for $\dot{Q}_{\mathrm{r},g-a}$ and $\dot{Q}_{\mathrm{c},g-a}$ Eq. (3.1), we get,

$$\dot{Q}_{g-a} = h_g\,\mathrm{A_g}(\mathrm{T_g} - \mathrm{T_{amb}}) \quad (3.2)$$

where,

$$h_g = h_{rg} + h_{cg} \quad (3.2.1)$$

Case (i); the empirical relation for h_g is given by Watmuff et al. (1977).

$$h_g = 5.7 + 3.8\,V \quad (3.2.2)$$

Where V is the wind Velocity in m/s. Eq. (3.2.2) includes the effect of convection (natural as well as forced) and radiation from the glass cover.

Case (ii); we can also evaluate the radiation and convection losses separately. Radiative losses we can calculate from Eq. (3.1.1) and convective heat transfer coefficient h_{cg} can be obtained from the relation.

$$h_{cg} = 2.8 + 3.0\,V \quad (3.2.3)$$

There is no significant change in the performance of the solar still if we evaluate h_g either by case (i) or case (ii).

Heat transfer from the Bottom and Side walls

Heat is also lost from the water in the basin to the ambient through the insulation and subsequently by convection and radiation from the bottom or side surface of the basin. The bottom loss coefficient (U_b) can be written as,

$$U_b = \left[\frac{1}{h_w} + \frac{1}{K_i / l_i} + \frac{1}{h_{rb} + h_{cb}}\right]^{-1} \quad (3.3)$$

The side heat loss coefficient (U_s) can be approximated as

$$U_s = U_b \times \frac{A_s}{A_h} \tag{3.4}$$

3.2.2. Internal Heat Transfer

The internal heat transfer i.e. heat exchange from the water surface to the glass cover inside the solar still is governed by radiation, convection and evaporation as shown in Fig. 3.2.

I. Radiative Heat transfer

In this case it was assumed that water surface and the glass cover are infinite parallel planes and thus shape factor between water and glass cover can be taken as unity. The expression for radiative heat loss from the water to inner glass surface can be written as

$$\dot{Q}_{r,w-g} = \varepsilon_w A_w \sigma[(T_w + 273)^4 + (T_g + 273)^4)] \tag{3.5}$$

$$\dot{Q}_{r,w-g} = h_{rw} A_w (T_w - T_g) \tag{3.5.1}$$

here h_{rw} is the radiative heat transfer coefficient from the water surface which can be written as,

$$h_{rw} = \varepsilon_w \sigma[(T_w + 273)^2 + (T_g + 273)^2][T_w + T_g + 546] \tag{3.5.2}$$

II. Convective Heat Transfer

Heat transfer occur across humid air within the solar still only by free convection, which is caused by buoyancy due to density difference which occurs due to the temperature gradient between water and vapours near the inner glass surface. The expression for convective heat transfer within the solar still can be given by,

$$\dot{Q}_{c,w-g} = h_{cw} A_w (T_w - T_g) \tag{3.6}$$

here h_{cw} is the convective heat transfer coefficient from the water surface which was derived by Dunkle (1961),

$$h_{cw} = 0.884\left[(T_w - T_g) + \frac{(P_w - P_g)(T_w + 273)}{268 \times 10^3 - P_w}\right]^{1/3} \tag{3.6.1}$$

III. Evaporative Heat transfer

It is the loss due to mass transfer in the form of water vapour from the water surface because of pressure difference i.e. $(P_w - P_g)$ corresponds to saturation pressure at water temperature and saturation pressure at glass temperature. The rate of evaporative heat transfer from the water surface to the glass cover can be written as,

$$\dot{Q}_{ew} = h_{ew} A_w (T_w - T_g) \tag{3.7}$$

Also, we can write the expression of $\dot{Q}_{ew}$ in terms of h_{cw} derived by Cooper (1973),

$$\dot{Q}_{ew} = 0.0162 h_{cw} A_w (P_w - P_g) \tag{3.7.1}$$

We can calculate the value of h_{ew} from Eq. (3.7) and (3.7.1) which is given by the expression,

$$h_{ew} = 16.273 \times 10^{-3} h_{cw} \frac{(P_w - P_g)}{(T_w - T_g)} \tag{3.7.2}$$

3.3. Heat and Mass Balance of Solar Still

The energy balance for the stills is carried out with the following assumptions for simplification:

i. Absorptivity of glass cover is neglected,
ii. Only natural convective heat loss from the side surfaces of the solar still are considered,
iii. Water level in the basin of the solar still is constant during the experiment,

The heat transfer mechanism in the solar still is given in Fig. 3.3. For energy balance, solar still is considered as an open system. Solar radiation that falls on the glass enter the solar still i.e. heat input, is equal to heat goes out of it i.e. heat transfer losses from its surfaces to the ambient/sky, heat transferred to evaporate the distilled water as well as to evaporate the unaccounted water which lost in form of vapor, heat transferred carried by the distilled water at temperature higher than that of feed water, and the amount of solar radiation which get reflected from the outer surface of the glass.

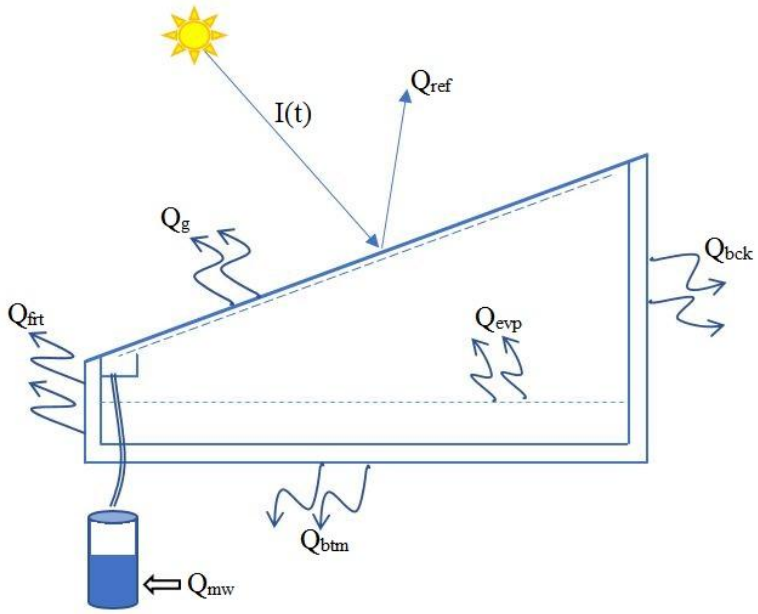

Figure 3.3: Heat Transfer Mechanism in Solar Still

Heat balance for the solar still

Heat In = Heat Out

Heat In: Incident solar radiation - Reflected solar radiation

Heat Out: Surfaces heat transfer loss + heat escaped from the system as distilled water + heat carried by the distilled water

I. Incident Solar Radiation

Incident solar radiation, $Q_{in} = I(t).\mathrm{A}_g$ (3.8)

II. Surfaces heat transfer loss

Heat transferred from the surfaces of solar still – glass surface, and other five walls (front, rear/back, right, left, and bottom) enclosing surfaces of Still.

a) Heat transfer from glass surface to sky; Q_g

i) Convective mode of Heat transfer b/w glass and sky; Q_{cg}

$$Q_{cg} = h_{cg}.\mathrm{A_g}.(\mathrm{T_g} - \mathrm{T_{sky}}) \quad (3.8.1)$$

whereas, h_{cg} taken from Sharshir S. W. et al,

$$h_{cg} = 5.7 + 3.8 \times V_a \quad (3.8.2)$$

The sky temp. taken from Sharshir S. W. et al,

$$T_{sky} = T_a - 6.0 \tag{3.8.4}$$

ii) Radiative mode of heat transfer b/w glass and sky; Q_{rg}

$$Q_{rg} = \varepsilon_g A_g \sigma((T_g + 273)^4 - (\mathrm{T_{sky}} + 273)^4) \tag{3.9}$$

b) Heat transfer from other five surfaces of the Still to its ambient;

Whereas, five surfaces – left side wall, right side wall, front wall, back wall, and bottom surface.

i) For left side wall heat transfer through convective mode; Q_{cL}

$$Q_{cL} = h_{cL} A_L (\mathrm{T_L} - \mathrm{T_a}) \tag{3.10}$$

whereas, h_{cL} is calculated through the Nusselt no. (N_u), i.e.; $h_{cL} = \frac{N_u.\mathrm{k}}{L_c}$.

The Nusselt no., N_u is calculated as:

<u>For vertical plate:</u>

$$N_u = \begin{cases} 0.59\ R_a^{1/4} & ;\ 10^4 < \mathrm{R_a} < 10^9 \\ 0.1\ R_a^{1/3} & ;\ 10^9 < \mathrm{R_a} < 10^{13} \end{cases} \tag{3.10.1}$$

<u>For horizontal plate:</u>

If upper surface is of hot plate;

$$N_u = \begin{cases} 0.54\ R_a^{1/4} & ;\ 10^4 < \mathrm{R_a} < 10^7 \\ 0.15\ R_a^{1/3} & ;\ 10^7 < \mathrm{R_a} < 10^{11} \end{cases} \tag{3.10.2}$$

If lower surface is of hot plate;

$$N_u = 0.27\ R_a^{1/4} \quad ;\ 10^5 < \mathrm{R_a} < 10^{11} \tag{3.10.3}$$

whereas, R_a is Raleigh no. which calculated by;

$$R_a = G_r.\mathrm{P_r} = \frac{g.\beta.(\mathrm{T_L} - \mathrm{T_a}).\mathrm{L_c}^3}{\nu^2}.\mathrm{P_r} \tag{3.10.4}$$

ii) For left side wall heat transfer through radiative mode; Q_{rL}

$$Q_{rL} = \varepsilon_L A_L ((\mathrm{T_L} + 273)^4 - (\mathrm{T_a} + 273)^4) \tag{3.11}$$

whereas, A_L is the area of the left side walls, T_L is the instantaneous temperature of left side surface which is being recorded every 15 min, ε_L is the emissivity of the left side wall surface.

So, total heat transferred from the left side wall is, $Q_L = Q_{cL} + Q_{rL}$

Similarly, calculation for heat transfer through convective or radiative mode of other remaining four walls (i.e. Q_R, Q_{bck}, Q_{btm}, Q_{frt}) would be same as per their respective areas, temperatures, orientation, and emissivity.

III. Heat transfer in Evaporation

Heat transferred in the evaporation of the distilled water as well that of water which is lost to the ambient as vapors; Q_{evp}

Total mass of water which undergoes evaporation = mass of distilled water + mass of vapor loss

$$M_w = m_w + m_v \tag{3.12}$$

$$Q_{evp} = M_w . h_{fg} \tag{3.13}$$

whereas, h_{fg} is taken from [6]; h_{fg} = 2335 kJ/kg,

IV. Heat carried by the distilled water:

Heat carried by the distilled water as the temperature of the outgoing water was higher than that of feed water; Q_{mw}

$$\Delta Q_{mw} = \Delta m_w . C_w . (T_w - T_{fw}) \tag{3.14}$$

whereas, T_{fw} is the initial temperature of feed water, and T_w is the instantaneous temperature of the distilled water which is been recorded within every 15 min.

$$Q_{mw} = \sum_{initial\ \text{state}}^{final\ \text{state}} (\Delta Q_{mw}) \tag{3.14.1}$$

V. Reflected Solar Radiation; Q_{ref}

Amount of reflected radiations from the outer surface of the glass, has been evaluated using Fresnel equations for reflection. Incident radiations is divided into two perpendicular components, s-polarized and p-polarized. There are two different

equations for the two components. Some of the radiation gets reflected from the outer surface and a part gets reflected from the inner glass surface. Reflection from both the surfaces have been accounted for. The total reflection from the glass surface is calculated with following assumptions, i.e.– interface surface is flat, media is homogeneous, and incident radiations is equally divided between two polarizing planes.

Fresnel equation for the reflectance is:

Reflectance for s-polarized light; R_s

$$R_s = \left| \frac{n_1 \cos\theta_i - \mathrm{n}_2 \cos\theta_\mathrm{t}}{n_1 \cos\theta_\mathrm{i} + \mathrm{n}_2 \cos\theta_t} \right|^2 \tag{3.15.1}$$

Reflectance for p-polarized light; R_p

$$R_p = \left| \frac{n_1 \cos\theta_t - \mathrm{n}_2 \cos\theta_\mathrm{i}}{n_1 \cos\theta_t + \mathrm{n}_2 \cos\theta_i} \right|^2 \tag{3.15.2}$$

whereas, n_1, n_2 are the refractive index of air and glass respectively, and θ_i, θ_t are angle of incident and refracted ray respectively, and θ_t is calculated by the Snell's Law, i.e., $n_1 \sin\theta_i = n_2 \sin\theta_t$

angle of incidence (θ_i) of the Sun on a surface tilted at an angle from the horizontal (β), when the surface is tilted towards the latitude of site (facing south in the northern hemisphere)

$$\cos\theta_i = \cos\delta\cos(\phi-\beta)\cos\omega + \sin\delta\sin(\phi-\beta) \tag{3.15.3}$$

where, δ is deflection angle, ϕ is latitude angle (i.e.26.8$^\mathrm{O}$), β is the surface tilted angle (i.e.26.8$^\mathrm{O}$) and ω is an hour angle which we have to calculate further for every hour according to IST.

Reflection of incident radiation from outer surface of glass is given by, R

$$R = \frac{R_s + R_p}{2} \tag{3.15.4}$$

Heat lost due the reflection; Q_{ref}

$Q_{ref} = \sum_{initial}^{final} \bar{I}.\bar{R}$; whereas $\bar{I}$ is an average solar intensity on the surface of glass for an hour, $\bar{R}$ is average reflectivity for an hour.

All the heat which are evaluated will be considered for heat balance;

$$Q_{in} = Q_g + Q_L + Q_R + Q_{bck} + Q_{btm} + Q_{frt} + Q_{evp} + Q_{mw} + Q_{ref} + Q_{un} \quad (3.16)$$

Chapter 4.
Experimental Setup

4.1. Major Components of Solar Still

4.1.1. Double Walled GI Sheet Basin

Solar still basin was made up of double walls of GI-sheet (24 gauge i.e. 0.511 mm) with base area of 0.98 m x 1.08 m. The thermal resistance and absorptivity of basin should be high. Thermocol of 1 inch thickness was used between the walls to reduce the conduction losses from the bottom and the side walls of the solar still. In order to increase the absorptivity of solar radiation the basin was painted black using synthetic black paint. Pouring of the raw water to the basin was through an inlet pipe. The stopper was used to tighten the inlet to avoid escaping of vapours.

4.1.2. Glass Cover

The Glass cover at the top of the basin, rested on the side walls frame which was at some inclination with horizontal. Cost of the material, weight, local availability, maximum temperature tolerance and impact resistance as well as its ability to transmit solar energy and infrared light are important factors to determine the suitability of the glazing material.

For the experimental setup, ordinary transparent glass was used having thickness of 5 mm. Inclination of the glass cover was kept at 26.8°, i.e. same as the latitude of the experimental site i.e. MNIT Jaipur (26.8613° N and 75.8140° E). Bio-foam sheet was used between the glass cover and the frame in order to seal the gaps between the glass sheet and the frame to prevent leakage of water vapours from the solar still.

4.1.3. Distillate Water Collector

Water collector was also made of GI-sheet. The water collector was fixed at the lower edge of the glass, just below the glass. There was a small glass strip fixed at the underside of the glass with the help of silicon gel. Its function was to prevent the water drops from sliding into the gap between the glass and the frame and force them to fall

into the collecting tray. Collector base was slightly inclined towards the outlet. This was provided to ensure smooth flow of the distillate water from collector to the outlet.

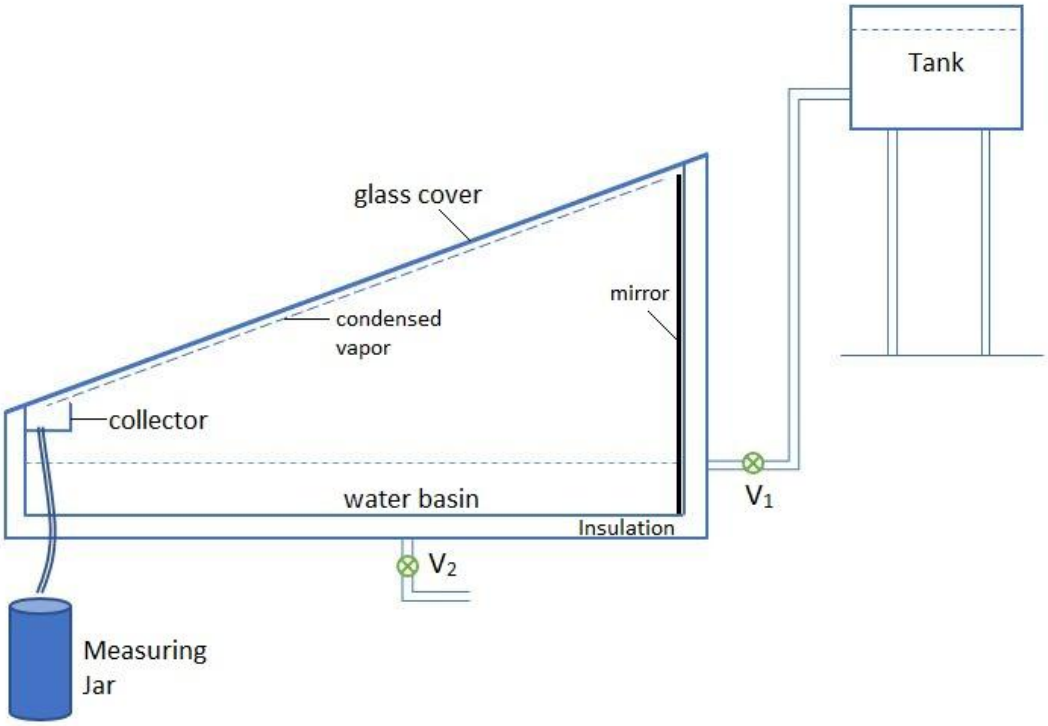

Figure 4.1: Schematic Diagram of Solar Still

4.1.4. Internal Reflectors

5 mm thick mirrors were used as internal reflectors as shown in Fig 4.1. In total, three mirrors were placed on the three side walls, while one small side wall where no radiations fall was left uncovered. The purpose of the internal mirrors was to reflect solar radiation that falls on the inner surface of the walls to the basin, and thereby prevent its loss from the side walls. Kabeel et al. (2013) has also done used internal mirrors to improve the performance of solar still.

4.2. Orientation of Solar Still

The orientation of the solar still was fixed to have the maximum solar radiation and minimum reflectivity throughout the day. For northern hemisphere region device is to be placed towards south facing direction as to have 180° azimuthal angle from the north, which helps in minimizing the reflectivity. Thus, the orientation of solar still was fixed towards south facing direction and this south direction was achieved using a compass.

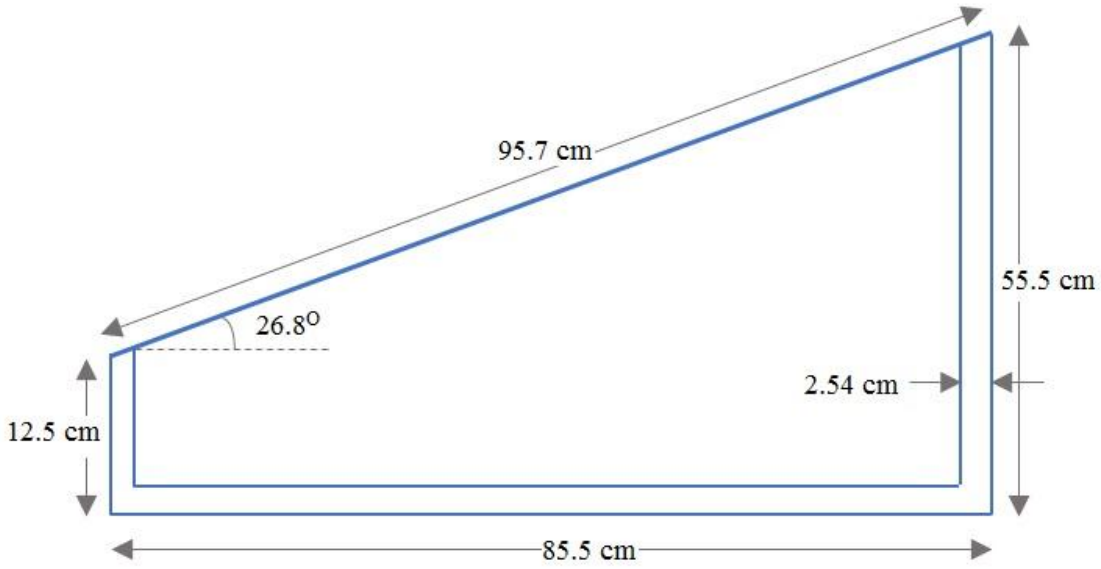

Figure 4.2: Dimensions of Solar Still Setup

4.3. Instruments Used

4.3.1. Solarimeter

Solarimeter was used to measure the global solar radiations received on the inclined surface to record the solar intensity. The top surface of the Solarimeter consists of a rectangular photo sensor. When sunlight falls on this photo sensor it is converted into electricity. Solarimeter measures global solar radiation which includes both direct as well as diffused solar radiation and displays the total radiation directly in watts per meter square.

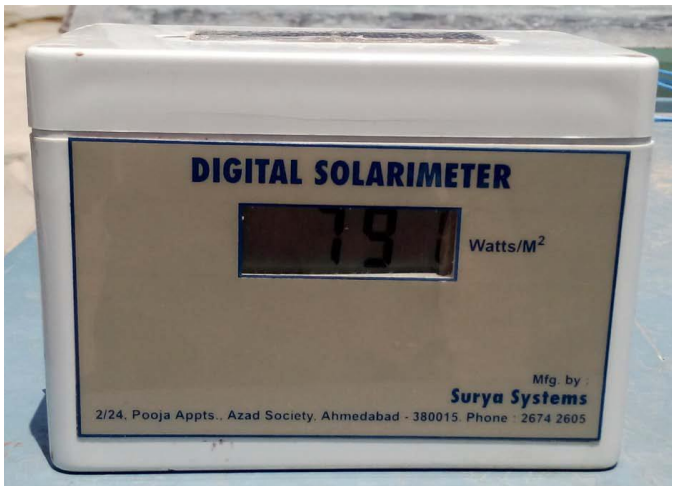

Figure 4.3: A Photo of Digital Solarimeter

4.3.2. Data Logger

Data logger is a device which automatically records the data within a desired interval of time and stores the data in the digital form. Data logger can store the measured data of the desired measurements like voltage, current, temperature, velocity, etc. Some of the data loggers have display unit and some have not. Display unit helps in making a preliminary check that the correct readings are being read by the data-logger.

Agilent data logger was used in the setup as shown in Fig. 4.4, to record the reading as well as display the desire data. Agilent data logger can scan data for AC and DC voltage both, and for temperature through all type thermocouples like J, K, S, T, L, M, N, etc. It can scan up to 9999 times, within an interval of one second, and in one scan can store data of 60 different sensors i.e. 20 units (thermocouples) per channel.

Figure 4.4: A Photo of a Aligent Data Logger

4.3.3. Thermocouples

There are several types of thermocouples for different temperature ranges, some of them are mentioned in Table 4.1.

Out of these thermocouples, on the basis of cost, operating temperature range and linearity, T-type thermocouples were chosen for the experiment.

Table 4.1: Composition, Temperature Ranges of the Thermocouples

Thermocouple Type	Conductors-Positive	Conductors-Negative	Temperature Range (°C)
B	Platinum-30% Rhodium	Platinum-6% Rhodium	400 to 1820
E (Chromel-Constantan)	Nickel-Chromium alloy	Copper-Nickel alloy	-200 to 1000
J (Iron-Constantan)	Iron	Copper-Nickel alloy	-200 to 1200
K (Chromel-Alumel)	Nickel-Chromium alloy	Nickel-Aluminum alloy	-200 to 1372
N (Nicrosil-Nisil)	Nickel-Chromium-Silicon alloy	Nickel-Silicon-Magnesium alloy	-200 to 1300
T (Copper-Constantan)	Copper	Copper-Nickel alloy	-200 to 400

Before using thermocouples for the experiment, they need to be calibrated. Two wires of T-type thermocouple were welded at one end, which was placed at the temperature sensing location, whereas other ends of the wire were connected to the digital indicator/ data logger. Twenty-Six T-type (copper-constantan) thermocouples were fixed to measure temperature at different locations. Four thermocouples were pasted on the outer surface of the glass, four on the inner surface of the glass, two in the water basin, two thermocouples were suspended in the vapour zone to measure vapour temperature,

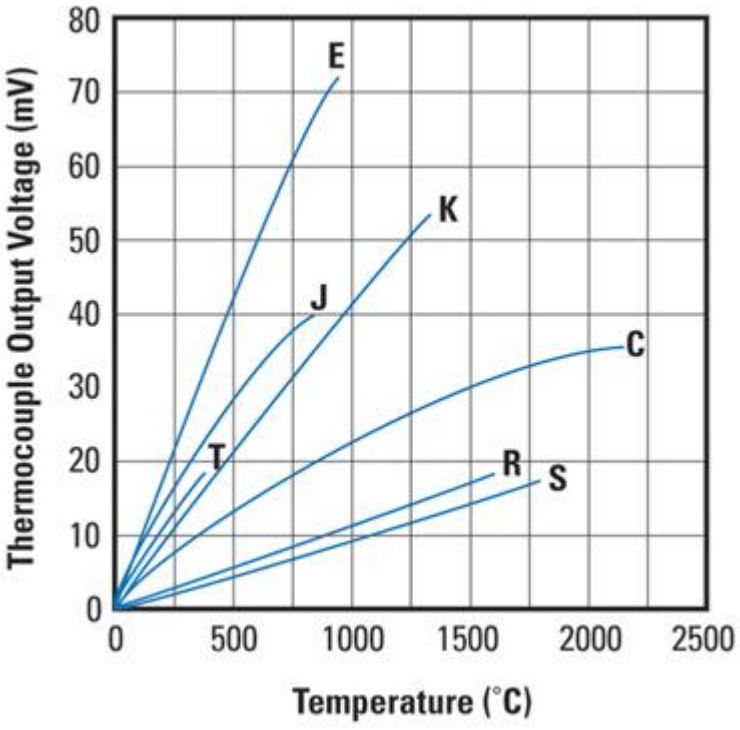

Figure 4.5: Thermocouples Linearity Curve Range

four thermocouples were pasted over the back wall, three each were pasted on the right and left side walls, and two thermocouples were placed outside in shade to measure ambient temperature, two over the front wall, and one at the outlet of distilled water. Temperature of thermocouples placed on one surface were averaged and the mean value was considered as a uniform temperature for that surface. Locations of thermocouples on the solar still are shown in Fig. 4.6.

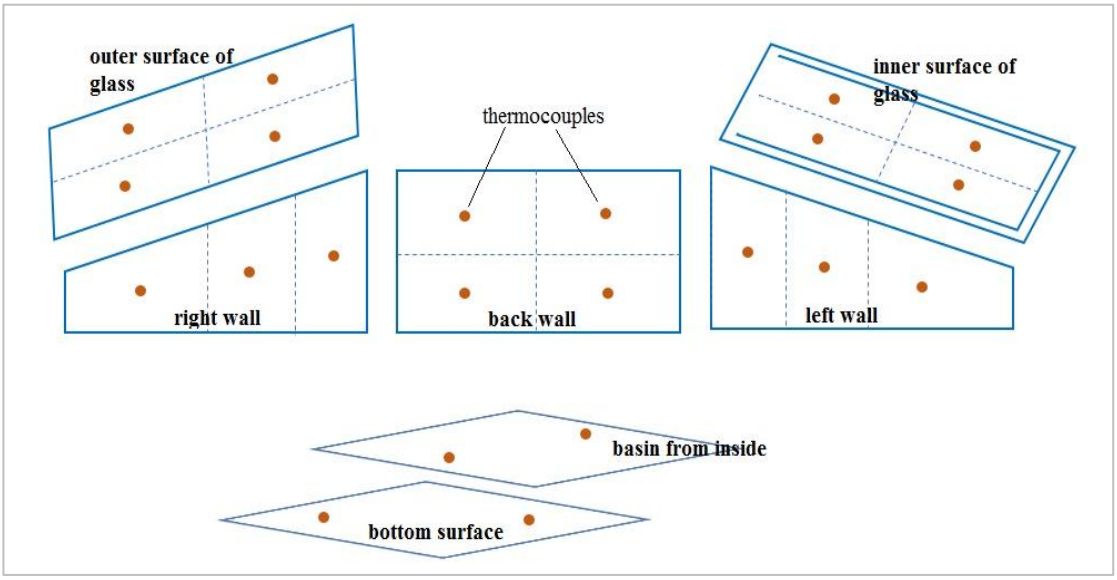

Figure 4.6: Location of Thermocouples

4.3.4. Fluke Oil Bath Calibrator

Digital calibrator is used to calibrate thermocouples. The calibration of thermocouples was done by Fluke oil bath calibrator. It consists of three units, first one is the Connector to which thermocouples are connected, the second is the Monitor with and a Control Keypad which displays the results, and the third one is an Oil Bath which raises or lowers the temperature of the oil bath as per the set points. Set points are those point at which thermocouples are calibrated. Thus, the set points were chosen within the expected operating range.

Accuracy and the errors associated with different instruments are given in Table 4.2.

Table 4.2: List of the Instruments used along with their Error (%)

S. No.	Instrument	Accuracy	Range	Error %
1.	Fluke Oil-bath Calibrator	± 0.0001	0-100 °C	0.01
2.	Agilent data logger	± 0.1°C	0-500 °C	-
3.	Solarimeter	± 1 W/m^2	0-2000 W/m^2	2.5
4.	Measuring Jar	± 10 ml	0-1000 ml	10

4.4. Calibration of Thermocouples

Calibration of the thermocouples was carried out using Fluke oil bath calibrator. It consists of three units, as mentioned before, and a Master sensor. Master sensor is an RTD which is used as reference. Calibration of the thermocouples was done at five set points, i.e. at 0°, 25°, 50°, 70°, and 90°C. In this apparatus twenty thermocouples can be calibrated simultaneously.

One end of thermocouples were connected to the Connector and the second ends were put in the Oil bath. The thermocouples type, no. of set points with temperature value of set point was fed in the system using Monitor device. After starting the calibration, oil temperature rises or falls according to the desired set points.

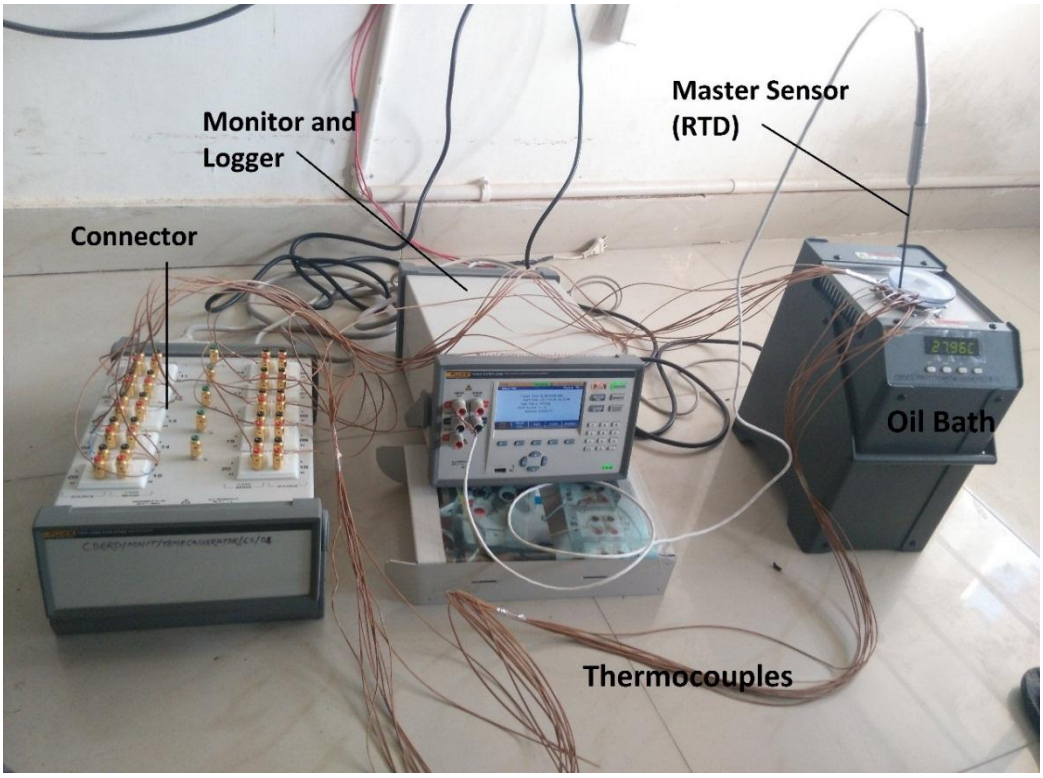

Figure 4.7: Fluke Oil Bath Calibrator

As oil reaches the set point temperatures, scanning of connected thermocouples temperature along with temperature of Master sensor starts. At each set point scanning take place five times. These scanned data can be taken out in a flash drive. Calibration of twenty-six thermocouples was carried out. The result of the calibration is given below in Table 4.2(a), (b), and (c). These reading are the average of the five scanned data at one set point.

Table 4.3(a): Calibration of T-Type Thermocouples (T_1 to T_{10})

T_{actual}	T_1	T_2	T_3	T_4	T_5	T_6	T_7	T_8	T_9	T_{10}
0.35	0.22	0.29	0.36	0.30	0.31	0.26	0.20	0.32	0.32	0.31
25.18	25.13	25.26	25.34	25.31	25.36	25.13	25.04	25.12	25.13	25.14
50.08	50.00	50.12	50.16	50.12	50.18	50.04	49.94	50.03	50.05	50.02
70.02	69.88	70.01	70.07	70.04	70.10	69.91	69.83	69.92	69.96	69.93
89.98	89.77	89.88	89.89	89.85	89.92	89.79	89.72	89.80	89.85	89.80

Table 4.3(b): Calibration of T-Type Thermocouples (T_{11} to T_{20})

T_{actual}	T_{11}	T_{12}	T_{13}	T_{14}	T_{15}	T_{16}	T_{17}	T_{18}	T_{19}	T_{20}
0.35	0.19	0.25	0.34	0.28	0.35	0.26	0.22	0.33	0.33	0.31
25.18	25.03	25.08	25.19	25.12	25.18	25.12	25.05	25.15	25.19	25.23
50.08	49.94	49.99	50.06	49.99	50.03	50.05	49.97	50.05	50.06	50.07
70.02	69.80	69.87	69.97	69.90	69.93	69.92	69.86	69.94	69.96	69.96
89.98	89.71	89.78	89.84	89.78	89.81	89.81	89.75	89.82	89.83	89.82

Table 4.3(c): Calibration of T-Type Thermocouples (T_{21} to T_{26})

T_{actual}	T_{21}	T_{22}	T_{23}	T_{24}	T_{25}	T_{26}
0.35	0.29	0.32	0.34	0.31	0.37	0.31
25.16	25.07	25.10	25.15	25.12	25.18	25.12
50.10	50.02	50.09	50.11	50.05	50.10	50.04
70.04	69.93	70.00	70.02	69.96	70.01	69.93
90.02	89.82	89.89	89.92	89.86	89.91	89.81

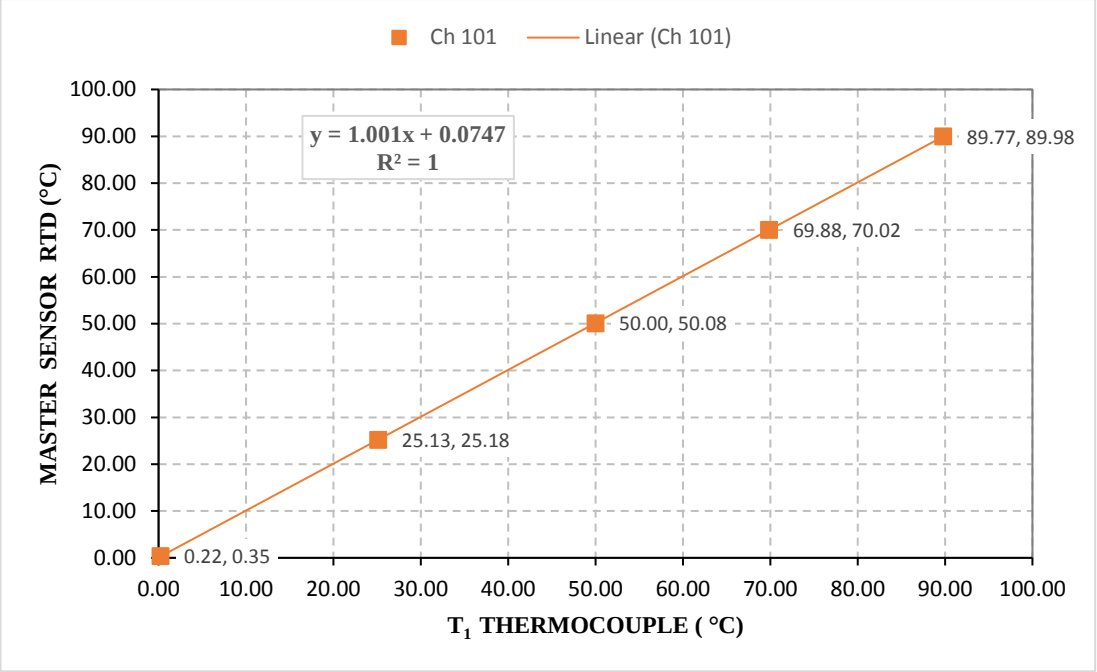

Figure 4.8(a): Variation of the T_1 Thermocouple with Master Sensor

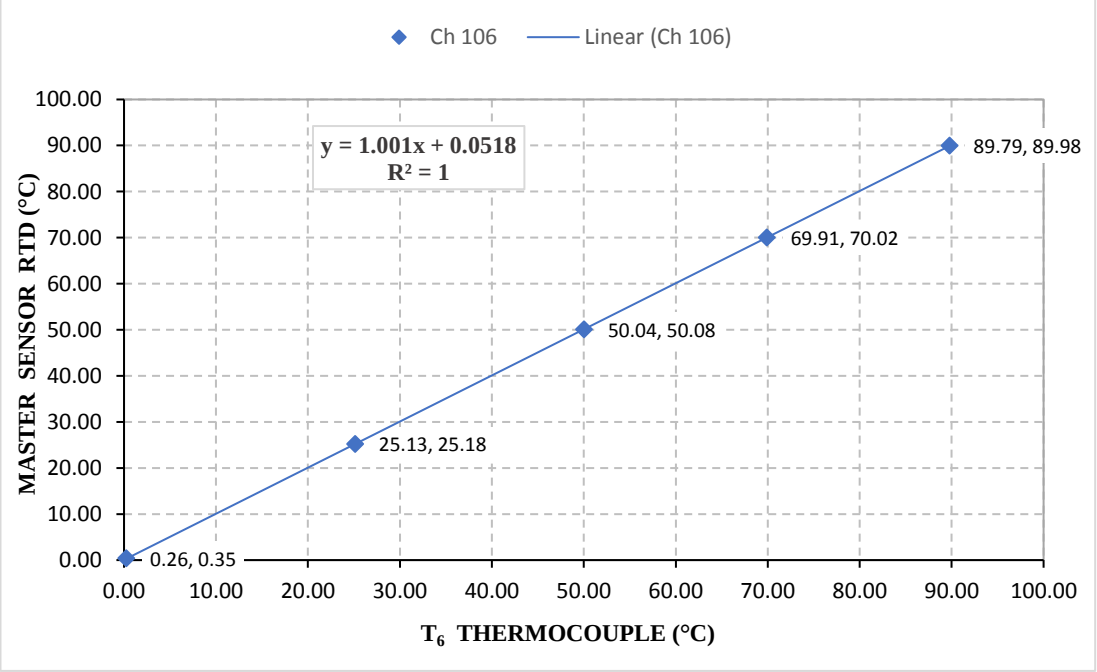

Figure 4.8(b): Variation of the T_6 Thermocouple with Master Sensor

Linear equations between actual and observed temperature for each thermocouple were developed. As a sample, equations for thermocouple T_1 and T_6, and the corresponding graphs are given below. In Fig 4.8(a) and (b).

$$T_{actual} = 1.001\ T_1 + 0.0747 \quad (4.2)$$

$$T_{actual} = 1.001\ T_6 + 0.0518 \quad (4.3)$$

Similarly, for all the twenty-six thermocouples similar equations were developed.

Chapter 5.
Experimentation

5.1. Procedure

For the heat and mass balancing of solar still following parameters were measured during the experimentation:

- temperature of inner and outer surface of glass, vapour, basin water, distilled water, side walls, back wall, front wall, bottom surface, and ambient.
- solar intensity,
- wind velocity,
- mass of distilled water output,
- mass of feed water before and after the experiment.

Temperature at various points was measured with the help of twenty-six T-type thermocouples which were connected to the Agilent data logger temperature scanner. Solarimeter was used to measure the solar intensity. Hourly measured wind velocity data was taken from MNIT Weather station network. The water quantity to be fed inside the solar still was measured using measuring cylinder of 1 l capacity. Before the experiment, measured quantity of water was supplied and the glass cover of solar still was cleaned. Distilled water output was measured with measuring cylinder of one litre. The mass of vapour escaped from the solar still was calculated using mass balance i.e. Sum of the mass of the water remaining in the basin of the solar still, mass of the distillate output collected in the measuring cylinder, and mass of the water vapour lost should be equal to the mass of water fed into the solar still before the start of the experiment. Reflectivity of the glass was evaluated for daylight hours from 8 a.m. to 6 p.m. Following observations were taken on hourly basis:

- Temperature of all the thermocouples,
- Solar intensity,
- Distillate output,
- Wind velocity.

5.2. Observations

Ten sets of experiments were done from 6th to 16th March, 2017. These experiments were carried out with the variation in feed water quantity, i.e. 10L, 15L, and 20L. On the basis of clear sky or minimal variation in solar intensity, six set of the experiments were selected, i.e. two sets of data for 10L, 15L, and 20L each, for the analysis. The experimental observations like solar intensity, distilled water output, wind velocity and temperature of all surfaces of solar still, water and vapour have been summarized in tabular form which are given below.

Table 5.1(a): Observation Data of the Temperatures (°C) on Date 06/03/17

Time (24hr)	T_{outer}	T_{Inner}	T_{rs}	T_{ls}	T_{bck}	T_{btm}	T_{wb}	T_{wv}	T_{amb}	T_{frt}
8	17.4	16.3	27.4	18.2	17.9	20.3	20.1	19.8	19.2	18.8
9	23.4	23.0	37.2	21.9	21.4	23.9	23.6	27.5	21.5	23.8
10	32.8	34.7	41.9	27.1	27.0	29.8	35.1	41.8	25.0	31.5
11	42.7	46.4	42.6	31.1	31.2	34.9	50.2	54.8	27.6	38.5
12	52.9	57.4	41.0	34.2	34.3	38.4	63.1	65.7	28.6	44.0
13	59.0	64.5	38.1	35.7	36.1	40.8	71.1	72.1	29.3	47.2
14	62.8	68.1	37.7	40.3	37.8	43.1	74.0	75.5	29.8	50.8
15	61.7	67.0	37.7	44.9	37.8	42.4	72.7	74.9	30.8	49.8
16	57.6	62.9	37.6	48.3	37.0	41.1	68.7	69.9	30.8	47.7
17	50.1	54.0	35.1	45.8	34.2	37.6	60.4	59.8	30.2	41.8
18	39.1	41.7	30.2	34.6	29.9	33.1	48.6	45.9	28.4	33.0

Table 5.1(b): Observation Data of Various Parameters on Date 06/03/17

Time (24hr)	Solar Intensity (W/m^2)	Productivity (ml)	Reflectivity (%)	Wind Velocity (m/s)
8	150	0	27.22	1.3
9	380	0	11.93	1.2
10	560	60	8.10	1.1
11	700	250	7.31	1.4
12	820	390	7.21	1.6
13	800	460	7.21	1.8
14	750	490	7.31	0.8
15	590	435	8.10	1.3
16	445	370	11.93	0.7
17	235	250	27.22	1.3
18	20	150	75.23	1.1
		(over night) 260		

Table 5.2(a): Observation Data of the Temperatures (°C) on Date

Time (24hr)	T_{outer}	T_{Inner}	T_{rs}	T_{ls}	T_{bck}	T_{btm}	T_{wb}	T_{wv}	T_{amb}	T_{frt}
8	20.6	20.0	29.2	21.6	22.2	22.4	20.3	23.9	22.4	21.9
9	22.7	23.0	29.3	23.0	23.0	23.9	23.9	27.4	22.4	24.0
10	31.2	32.4	37.5	26.8	26.7	29.2	34.3	39.0	24.8	30.8
11	42.4	45.1	40.7	31.4	31.4	34.2	49.5	53.8	27.2	37.8
12	51.1	55.2	39.7	35.1	35.1	37.7	61.7	63.3	29.4	41.8
13	53.0	58.1	36.8	36.3	36.2	37.9	68.3	66.5	29.8	41.5
14	56.0	61.0	36.9	40.0	37.5	40.0	70.2	71.5	31.1	44.8
15	55.9	61.1	36.6	41.8	37.1	39.3	69.3	69.1	30.7	43.6
16	52.6	57.2	35.6	43.1	35.7	38.1	63.8	64.0	30.5	41.9
17	47.3	50.7	34.3	42.8	33.9	36.4	57.0	56.0	30.7	38.4
18	37.6	40.1	29.8	33.2	29.5	32.2	47.0	44.0	28.5	31.7

Table 5.2(b): Observation Data of Various Parameters on Date 07/03/17

Time (24hr)	Solar Intensity (W/m^2)	Productivity (ml)	Reflectivity (%)	Wind Velocity (m/s)
8	160	0	27.19	1.6
9	310	0	11.92	1.3
10	525	20	8.10	1.1
11	620	140	7.31	1.0
12	805	340	7.21	1.5
13	790	390	7.21	1.2
14	737	410	7.31	1.8
15	575	370	8.10	1.4
16	430	330	11.92	1.6
17	220	210	27.19	1.2
18	25	120	75.20	1.3
		(over night) 220		

Table 5.3(a): Observation Data of the Temperatures (°C) on Date 11/03/17

Time (24hr)	T_{outer}	T_{Inner}	T_{rs}	T_{ls}	T_{bck}	T_{btm}	T_{wb}	T_{wv}	T_{amb}	T_{frt}
8	16.6	17.2	29.1	16.5	16.7	17.0	16.2	21.6	15.4	17.2
9	21.3	21.8	33.7	18.9	19.0	20.0	20.6	27.4	17.2	21.1
10	29.8	31.6	37.6	23.0	23.3	25.3	36.3	41.7	19.5	28.6
11	38.7	41.6	37.6	26.5	26.9	29.9	47.5	51.7	21.9	35.5
12	47.5	51.9	35.4	29.3	29.6	33.7	59.6	61.2	23.9	40.7
13	53.0	58.1	32.5	31.5	31.2	35.2	65.8	66.5	25.3	42.7
14	52.5	57.6	31.5	34.1	31.3	34.6	68.5	69.9	25.5	40.8
15	50.5	55.3	31.4	37.7	31.1	33.8	63.6	65.8	25.7	40.0

Time (24hr)	T_{outer}	T_{Inner}	T_{rs}	T_{ls}	T_{bck}	T_{btm}	T_{wb}	T_{wv}	T_{amb}	T_{frt}
16	46.0	50.7	30.1	36.8	29.3	32.3	59.0	59.4	25.0	36.6
17	39.2	43.0	27.9	37.4	26.9	30.1	51.4	48.8	24.4	33.2
18	30.7	33.7	23.3	26.4	23.1	26.5	42.3	37.7	22.6	25.5

Table 5.3(b): Observation Data of various parameters on Date 11/03/17

Time (24hr)	Solar Intensity (W/m^2)	Productivity (ml)	Reflectivity (%)	Wind Velocity (m/s)
8	180	0	27.08	0.8
9	340	0	11.87	0.7
10	490	0	8.08	0.7
11	610	80	7.30	1.1
12	740	270	7.21	1.0
13	790	390	7.21	1.5
14	740	450	7.30	1.6
15	630	410	8.08	1.5
16	430	345	11.87	1.6
17	230	250	27.08	1.5
18	40	155	75.11	0.8
		(over night) 400		

Table 5.4(a): Observation Data of the Temperatues (°C) on Date 12/03/17

Time (24hr)	T_{outer}	T_{inner}	T_{rs}	T_{ls}	T_{bck}	T_{btm}	T_{wb}	T_{wv}	T_{amb}	T_{frt}
8	15.6	15.0	34.6	17.3	18.0	18.3	14.9	18.0	18.4	17.6
9	20.0	20.0	36.2	20.0	19.8	21.6	18.0	23.2	19.4	22.1
10	28.2	29.5	38.5	24.3	24.0	26.9	26.7	34.6	21.6	29.8
11	35.5	38.2	37.5	27.7	27.0	30.6	49.7	45.0	23.3	35.8
12	43.7	47.7	35.6	30.2	30.2	34.1	52.4	55.1	24.7	40.2
13	50.8	55.8	33.3	31.9	31.7	36.3	61.8	62.8	25.5	44.3
14	55.3	61.2	32.9	36.4	33.1	37.7	67.0	67.3	26.3	45.5
15	55.8	62.0	33.2	40.4	32.9	37.3	68.0	68.2	27.0	44.4
16	52.9	58.9	32.2	43.8	31.5	35.9	65.2	65.6	25.6	42.7
17	48.1	52.0	30.7	42.4	29.7	33.7	59.0	56.1	25.6	36.9
18	38.3	42.1	26.0	32.1	25.7	29.3	49.7	44.4	23.5	29.3

Table 5.4(b): Observation Data of Various Parameters on Date 12/03/17

Time (24hr)	Solar Intensity (W/m^2)	Productivity (ml)	Reflectivity (%)	Wind Velocity (m/s)
8	190	0	27.05	0.7
9	450	0	11.85	0.9
10	610	20	8.07	1.1
11	690	30	7.30	1.4
12	760	150	7.21	1.4
13	790	290	7.21	1.5
14	690	390	7.30	1.6
15	580	450	8.07	1.3
16	430	450	11.85	1.4
17	230	350	27.05	1.5
18	0	200	75.09	0.8
		(over night) 495		

Table 5.5(a): Observation Data of the Temperatures (°C) on Date 15/03/17

Time (24hr)	T_{outer}	T_{inner}	T_{rs}	T_{ls}	T_{bck}	T_{btm}	T_{wb}	T_{wv}	T_{amb}	T_{frt}
8	19.5	19.7	27.9	20.2	20.8	21.5	19.9	21.1	21.0	21.3
9	23.1	23.8	34.1	23.0	23.1	24.5	22.9	24.7	22.3	24.8
10	31.2	33.1	38.8	27.2	27.5	29.2	30.8	35.5	25.1	31.0
11	39.9	43.2	39.8	30.9	31.0	33.1	43.2	47.2	26.8	36.6
12	49.1	53.7	39.3	33.4	34.2	36.3	54.7	58.1	28.2	41.8
13	56.5	61.9	38.4	36.7	36.8	40.3	63.3	66.4	30.0	47.5
14	60.6	66.4	38.4	41.2	38.2	42.0	68.7	70.5	30.8	49.7
15	59.7	65.7	38.3	43.9	38.0	40.7	66.4	67.9	30.9	47.8
16	57.0	62.0	38.1	47.3	37.5	40.2	62.0	62.3	31.6	46.2
17	51.9	55.9	36.4	47.0	36.1	38.4	59.2	58.0	31.3	42.4
18	42.7	45.8	31.8	37.0	31.6	34.7	50.7	47.6	29.4	35.1

Table 5.5(b): Observation Data of Various Parameter on Date 15/03/17

Time (24hr)	Solar Intensity (W/m^2)	Productivity (ml)	Reflectivity (%)	Wind Velocity (m/s)
8	150	0	27.00	1.1
9	380	0	11.83	1.2
10	540	0	8.06	0.6
11	690	70	7.30	1.4
12	820	255	7.21	1.4
13	770	400	7.21	1.5
14	710	460	7.30	1.7
15	610	420	8.06	1.4

Time (24hr)	Solar Intensity (W/m^2)	Productivity (ml)	Reflectivity (%)	Wind Velocity (m/s)
16	435	355	11.83	1.2
17	235	280	27.00	1.0
18	20	155	75.04	0.9
		(over night) 400		

Table 5.6(a): Observation Data of The Temperatures (°C) on Date 16/03/17

Time (24hr)	T_{outer}	T_{inner}	T_{rs}	T_{ls}	T_{bck}	T_{btm}	T_{wb}	T_{wv}	T_{amb}	T_{frt}
8	21.3	20.4	35.1	24.0	24.7	24.0	19.4	22.9	24.3	23.4
9	24.8	24.4	35.6	26.2	26.7	26.3	22.3	27.3	25.1	26.9
10	32.6	33.1	42.1	30.6	31.6	31.8	29.0	34.8	28.2	34.4
11	39.9	41.8	42.7	32.6	33.0	35.3	42.3	45.8	29.5	39.4
12	48.2	51.4	41.9	35.6	36.1	38.5	52.7	55.5	30.8	44.4
13	55.0	59.7	40.2	38.3	38.7	41.2	62.0	64.0	32.3	47.5
14	57.0	62.1	39.6	40.6	38.7	41.9	64.9	65.9	32.5	47.7
15	54.4	58.8	38.5	42.7	37.8	40.6	61.8	62.4	32.4	45.6
16	51.7	55.6	37.6	43.1	37.4	39.6	58.9	58.8	32.4	43.6
17	46.4	50.1	35.3	40.2	35.1	37.2	53.9	52.8	31.3	39.3
18	39.2	42.3	31.0	33.2	30.9	33.3	47.7	44.4	29.2	33.3

Table 5.6(b): Observation Data of Various Parameter on Date 16/03/17

Time (24hr)	Solar Intensity (W/m^2)	Productivity (ml)	Reflectivity (%)	Wind Velocity (m/s)
8	210	0	26.98	1.0
9	380	0	11.82	1.4
10	620	0	8.06	2.0
11	690	50	7.30	1.5
12	750	100	7.21	1.3
13	790	310	7.21	2.1
14	340	530	7.30	1.2
15	620	230	8.06	1.5
16	340	340	11.82	1.1
17	260	200	26.98	1.0
18	44	140	75.03	1.2
		(over night) 500		

5.3. Calculated data for Heat and Mass Balance

Calculated heat transfer across various surfaces for the day is shown in tabular form below.

Table 5.7(a): Hourly Heat (kJ) Transfer on Date 06/03/17

Time	Q_g	Q_{rs}	Q_{ls}	Q_{bck}	Q_{frt}	Q_{btm}	Q_{evp}	Q_{wm}	Q_{ref}
8-9	34.0	111.4	1.7	-1.0	6.4	24.8	0.0	0.0	125.5
9-10	139.6	96.2	9.3	16.2	18.0	47.5	140.1	2.7	132.1
10-11	295.9	85.4	17.2	31.7	33.9	78.1	583.8	21.7	140.6
11-12	488.8	64.8	26.7	49.5	47.3	103.7	910.7	50.4	160.6
12-13	607.0	41.8	31.2	61.5	55.7	121.9	1074.1	71.2	170.0
13-14	679.4	39.9	59.7	73.3	68.2	147.3	1144.2	83.6	163.8
14-15	613.3	31.2	79.9	58.0	56.9	115.8	1015.7	72.1	149.4
15-16	510.2	33.3	102.3	53.1	49.2	105.1	864.0	55.0	146.9
16-17	356.3	21.0	89.1	31.0	32.9	72.9	583.8	29.4	170.4
17-18	160.1	5.4	26.2	8.6	9.3	40.2	350.3	10.7	115.0
Over night							607.1		

Table 5.7(b): Hourly Heat (kJ) Transfer on Date 07/03/17

Time	Q_g	Q_{rs}	Q_{ls}	Q_{bck}	Q_{frt}	Q_{btm}	Q_{evp}	Q_{wm}	Q_{ref}
8-9	5.4	41.3	2.6	4.7	4.3	14.9	0.0	0.0	117.1
9-10	118.6	80.4	9.3	15.8	17.3	44.7	46.7	0.9	115.7
10-11	292.0	73.9	20.1	37.1	31.5	72.9	326.9	13.1	127.9
11-12	424.6	51.6	27.8	51.5	35.8	85.0	793.9	45.4	150.5
12-13	444.8	34.1	32.0	58.3	33.5	81.3	910.7	53.8	167.4
13-14	493.6	27.1	48.2	56.7	41.1	91.1	957.4	63.1	161.3
14-15	490.1	27.9	60.4	55.5	36.7	87.5	864.0	52.5	146.2
15-16	413.6	22.5	69.9	40.9	31.4	73.3	770.6	45.0	142.4
16-17	290.1	14.8	70.6	22.2	20.5	52.4	490.4	24.0	161.7
17-18	131.1	4.0	15.6	5.9	5.7	31.7	280.2	8.8	114.4
Over night							513.7		

Table 5.7(c): Hourly Heat (kJ) Transfer on Date 11/03/17

Time	Q_g	Q_{rs}	Q_{ls}	Q_{bck}	Q_{frt}	Q_{btm}	Q_{evp}	Q_{wm}	Q_{ref}
8-9	74.4	116.5	8.3	16.4	11.3	30.0	0.0	0.0	129.7
9-10	178.7	103.4	15.3	30.4	26.2	55.5	0.0	0.0	116.4
10-11	318.1	85.8	21.6	42.8	41.4	80.7	186.8	7.6	122.5
11-12	464.2	59.4	26.9	51.3	53.0	104.4	630.5	35.6	142.5
12-13	546.7	32.7	31.0	51.5	53.4	102.4	910.7	60.4	160.6
13-14	514.4	26.8	43.7	47.0	43.3	87.3	1050.8	68.8	161.6

Time	Q_g	Q_{rs}	Q_{ls}	Q_{bck}	Q_{frt}	Q_{btm}	Q_{evp}	Q_{wm}	Q_{ref}
14-15	463.0	28.1	67.3	45.6	41.9	79.5	957.4	59.2	152.7
15-16	370.2	23.5	57.2	34.0	29.2	68.6	805.6	43.3	148.4
16-17	239.5	13.4	67.2	15.8	21.5	50.5	583.8	24.3	164.9
17-18	110.7	1.1	8.4	0.8	4.2	31.8	361.9	9.6	134.4
Over night							934		

Table 5.7(d): Hourly Heat (kJ) Transfer on Date 12/03/17

Time	Q_g	Q_{rs}	Q_{ls}	Q_{bck}	Q_{frt}	Q_{btm}	Q_{evp}	Q_{wm}	Q_{ref}
8-9	11.8	119.3	2.8	3.5	7.9	23.4	0.0	0.0	152.5
9-10	114.0	97.5	12.4	19.5	23.8	53.0	46.7	1.1	149.4
10-11	221.1	75.5	20.6	29.5	37.6	71.6	70.1	2.6	145.0
11-12	361.2	54.6	25.7	48.3	47.3	96.0	350.3	18.1	153.1
12-13	501.5	36.5	30.4	53.9	59.5	112.5	677.2	43.5	162.7
13-14	584.7	32.9	57.6	63.1	60.7	122.3	910.7	65.8	156.2
14-15	566.0	30.8	78.2	49.9	54.3	107.1	1050.8	76.9	141.5
15-16	526.6	32.0	109.2	49.9	51.3	104.9	1050.8	71.4	142.4
16-17	397.3	20.4	92.6	28.1	27.5	73.6	817.3	48.6	164.8
17-18	235.3	8.6	34.0	13.8	12.3	49.6	467.0	19.6	90.6
Over night							1155.8		

Table 5.7(e): Hourly Heat (kJ) Transfer on Date 15/03/17

Time	Q_g	Q_{rs}	Q_{ls}	Q_{bck}	Q_{frt}	Q_{btm}	Q_{evp}	Q_{wm}	Q_{ref}
8-9	14.2	78.7	3.1	6.0	6.8	22.3	0.0	0.0	124.4
9-10	107.6	75.8	9.0	19.6	15.9	38.7	0.0	0.0	128.8
10-11	249.3	71.1	20.3	37.6	29.1	64.9	163.5	7.0	136.7
11-12	409.8	56.8	25.1	54.0	41.1	83.3	595.4	35.2	159.4
12-13	540.5	42.0	35.5	63.5	56.9	112.2	934.0	67.7	166.9
13-14	610.1	40.0	59.4	69.3	61.0	122.9	1074.1	85.7	156.2
14-15	562.1	34.7	70.4	59.3	49.0	94.5	980.7	76.8	147.0
15-16	495.1	33.1	99.5	51.4	45.8	93.9	828.9	60.9	146.5
16-17	374.9	22.1	86.5	38.4	29.6	68.0	653.8	42.1	167.3
17-18	212.6	7.9	30.2	12.4	11.7	46.8	361.9	17.3	114.2
Over night							934.0		

Table 5.7(f): Hourly Heat (kJ) Transfer on Date 16/03/17

Time	Q_g	Q_{rs}	Q_{ls}	Q_{bck}	Q_{frt}	Q_{btm}	Q_{evp}	Q_{wm}	Q_{ref}
8-9	-5.0	69.0	5.1	14.4	4.9	11.8	0.0	0.0	147.9
9-10	75.2	76.5	10.2	28.0	16.9	34.2	0.0	0.0	138.2
10-11	190.4	70.1	14.0	28.9	28.1	57.3	116.8	4.3	146.1

Time	Q_g	Q_{rs}	Q_{ls}	Q_{bck}	Q_{frt}	Q_{btm}	Q_{evp}	Q_{wm}	Q_{ref}
11-12	341.0	59.2	24.3	47.8	42.9	83.4	233.5	12.0	152.0
12-13	452.8	37.6	30.7	58.8	46.2	92.3	723.9	46.5	161.6
13-14	487.4	36.3	43.9	55.2	48.0	99.8	1237.6	89.5	119.0
14-15	419.2	29.9	60.8	47.9	41.0	84.2	537.1	39.3	108.9
15-16	349.5	24.1	52.7	42.5	28.2	68.6	793.9	54.0	131.3
16-17	257.0	15.8	41.1	27.1	18.9	52.8	467.0	27.8	160.6
17-18	154.3	5.8	14.9	9.9	8.2	35.2	326.9	13.7	150.2
Over night							1167.5		

Chapter 6.
Results and Discussion

On the basis of six-day experimental data, calculation for heat balance was carried out. Energy lost through reflection of solar radiation, energy carried away by distilled water, and energy lost due to leakage of vapour have been calculated and the same have been discussed through a heat balance chart.

6.1. Energy Lost through Reflection of Solar Radiation

Reflection of solar radiation from the glass surface was one of the major heat loss. Reflection of the solar radiation depends on the angle of incidence, refractive index of the glass used, and the hourly average solar radiation that falls on the glass of solar still.

Following six graphs Fig. 6(a) – (f) have been plotted for reflectivity, solar intensity, effective solar radiation and energy lost through reflection of solar radiation in variation with time. The graphs show that minimum variation in reflectivity was from 10 am to 3 pm and maximum reflectivity was at 6 pm = 75%. This is due to the change in angle of incidence of the solar intensity, as the angle of incidence decreases reflectivity falls down. The variation in reflectivity among the six days of experiment is very small. This is because of very small change (i.e. 6.3° to 2.4°) in the declination angle of Sun from 6^{th} to 16^{th} March.

Energy loss due to reflectivity depends on the solar intensity and the reflectivity. The peaks in the reflective energy loss are away from the peaks of solar intensity because loss depends upon the product of solar intensity and the reflectivity. Overall Reflective heat loss is about 9% of total solar intensity that falls on the surface of the glass.

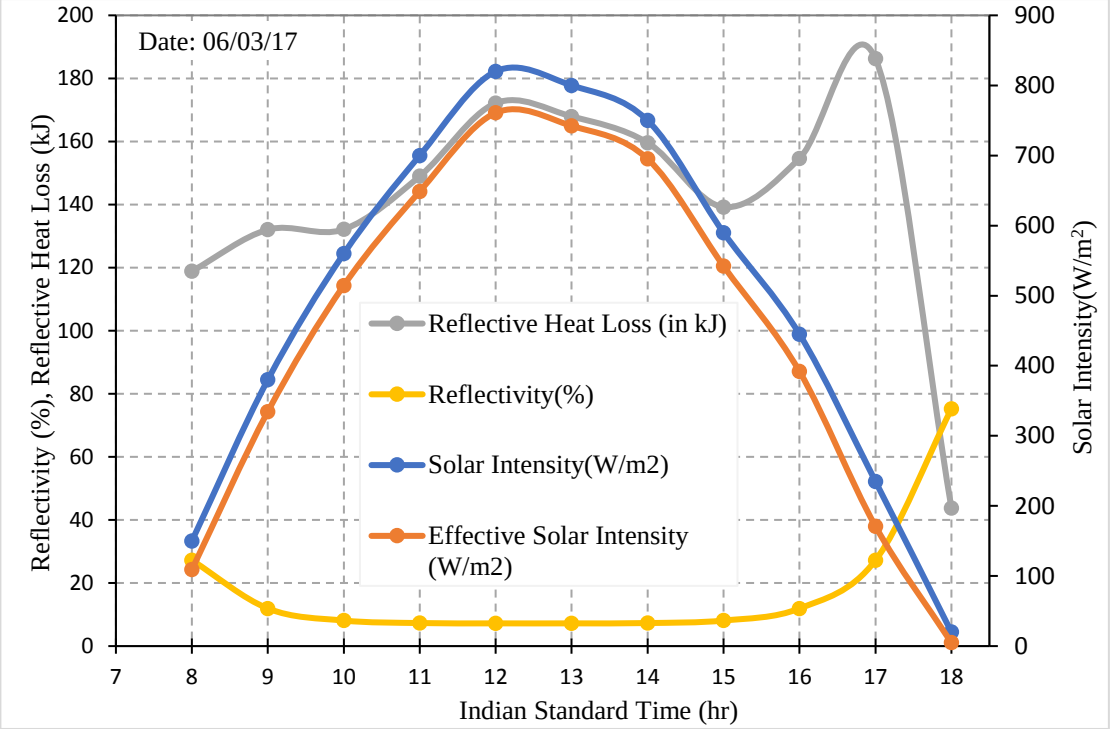

Figure 6.1(a): Hourly Variation of Energy Loss(kJ) due to reflectivity on Date 06/03/17

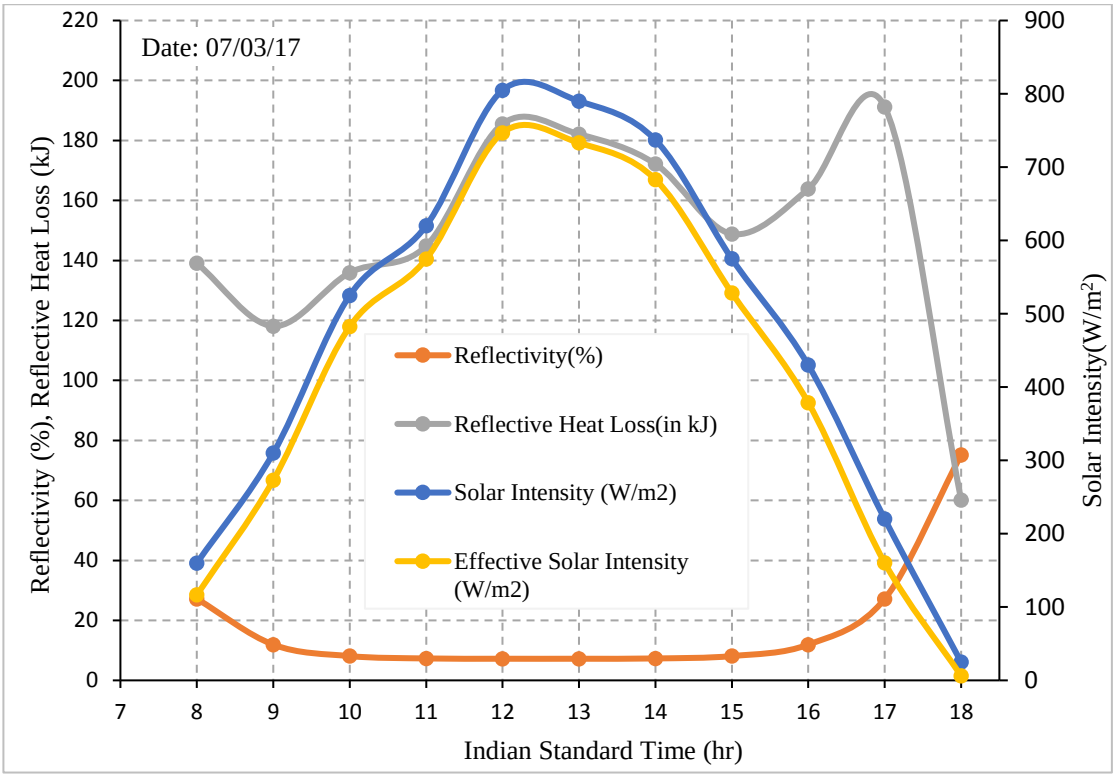

Figure 6.1(b): Hourly Variation of Energy Loss(kJ) due to reflectivity on Date 07/03/17

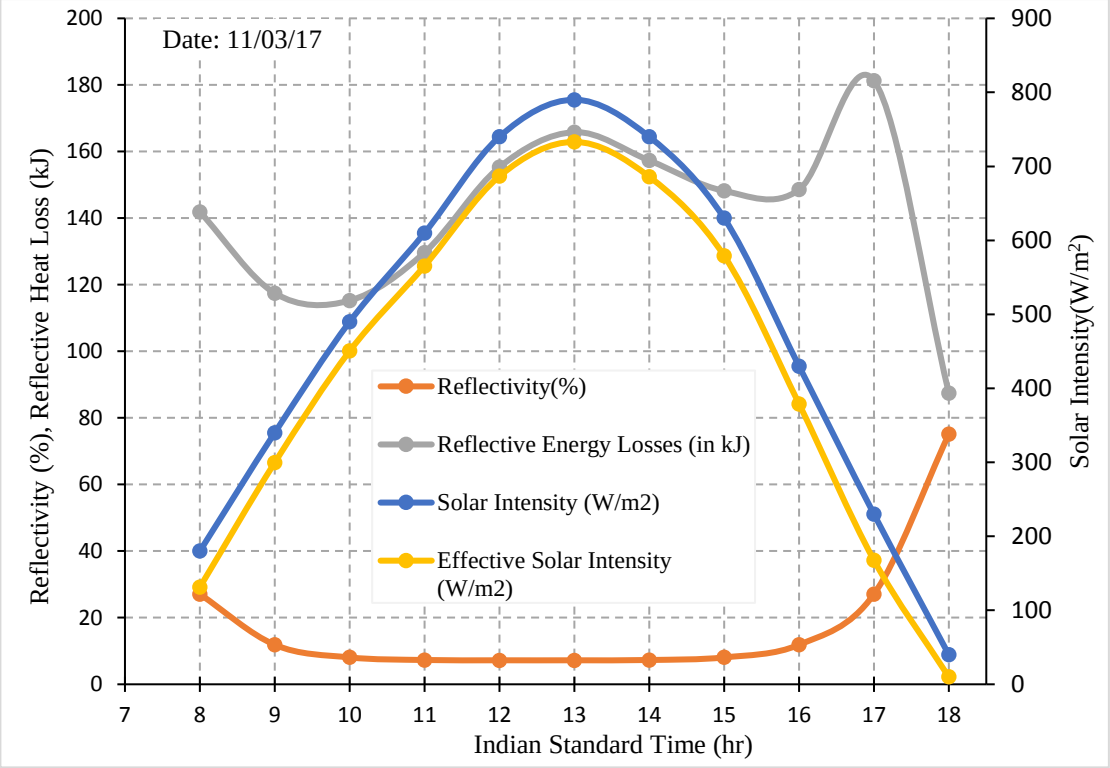

Figure 6.1(c): Hourly Variation of Energy Loss(kJ) due to reflectivity on Date 11/03/17

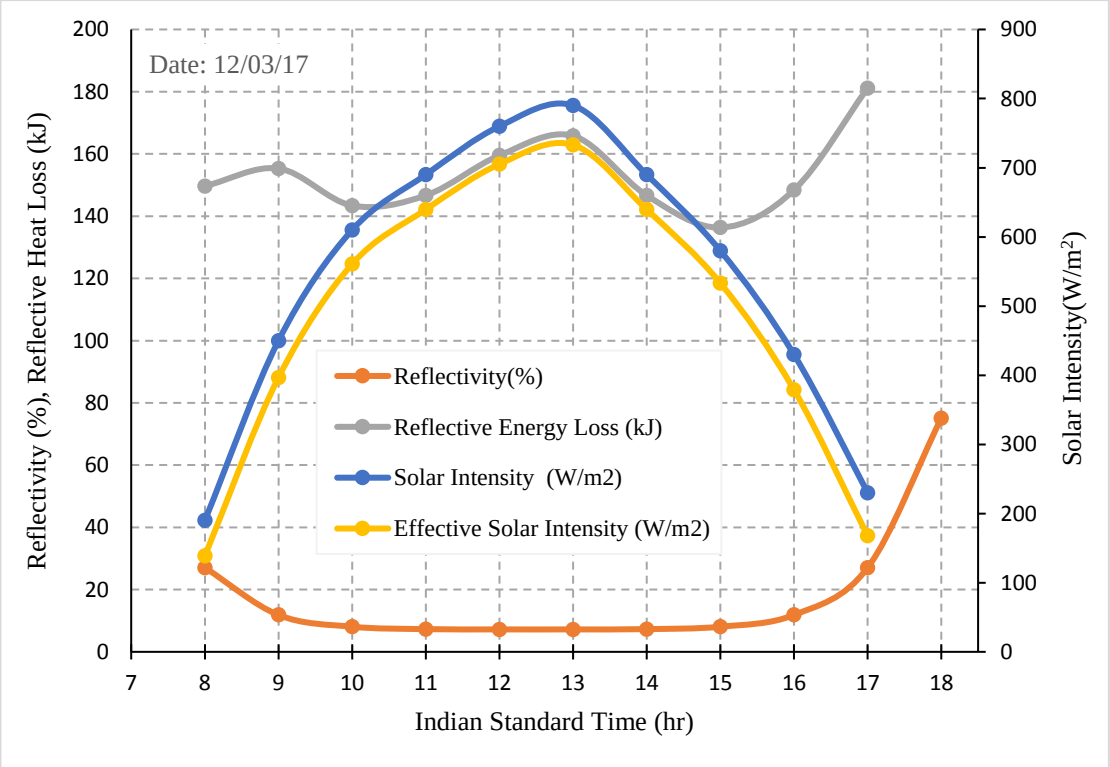

Figure 6.1(d): Hourly Variation of Energy Loss(kJ) due to reflectivity on Date 12/03/17

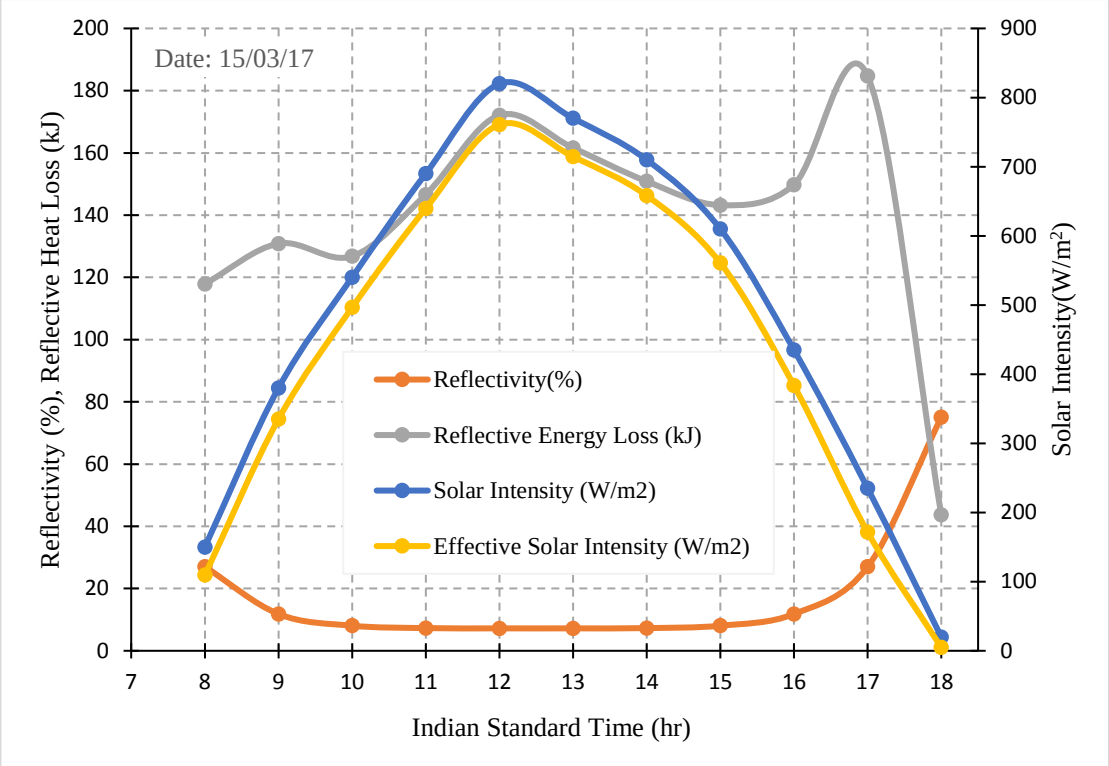

Figure 6.1(e): Hourly Variation of Energy Loss(kJ) due to reflectivity on Date 15/03/17

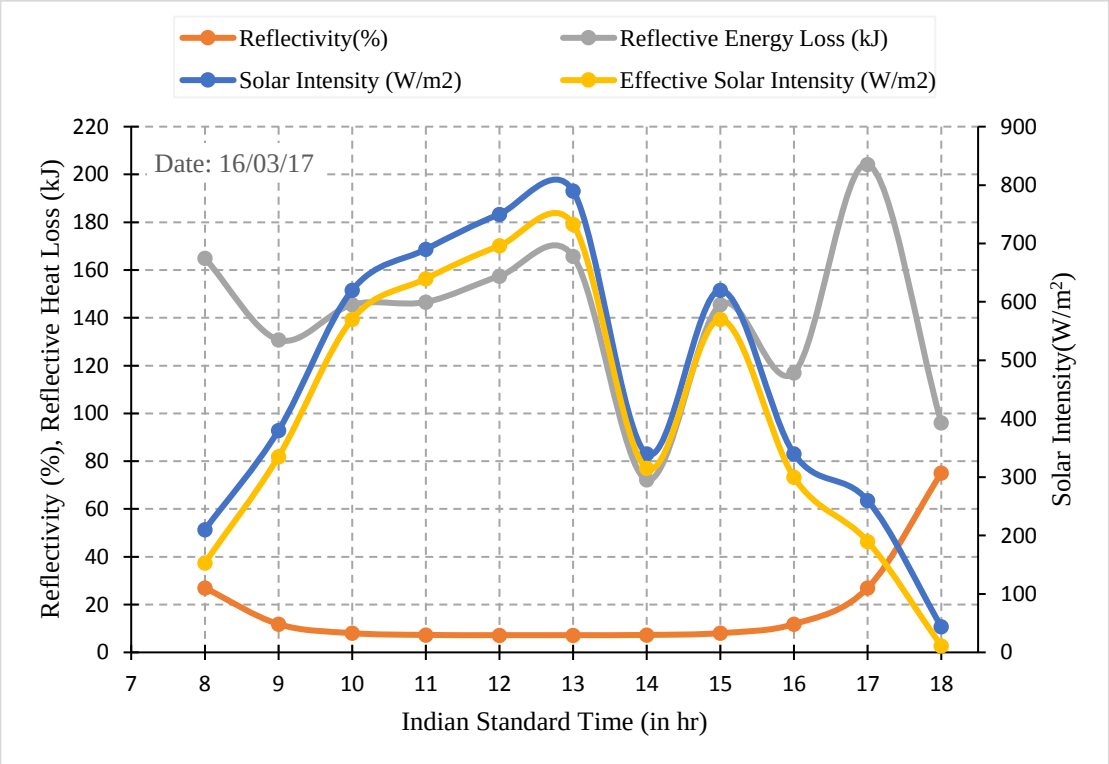

Figure 6.1(f): Hourly Variation of Energy Loss(kJ) due to reflectivity on Date 16/03/17

6.2. Energy Lost as Heat Content in Distilled Water

Amount of heat that is carried away with the distilled water is also accounted in the analysis. This heat loss is due to production the distilled water at the higher temperature. This is heat loss cannot be minimize, but can be utilized for other purposes.

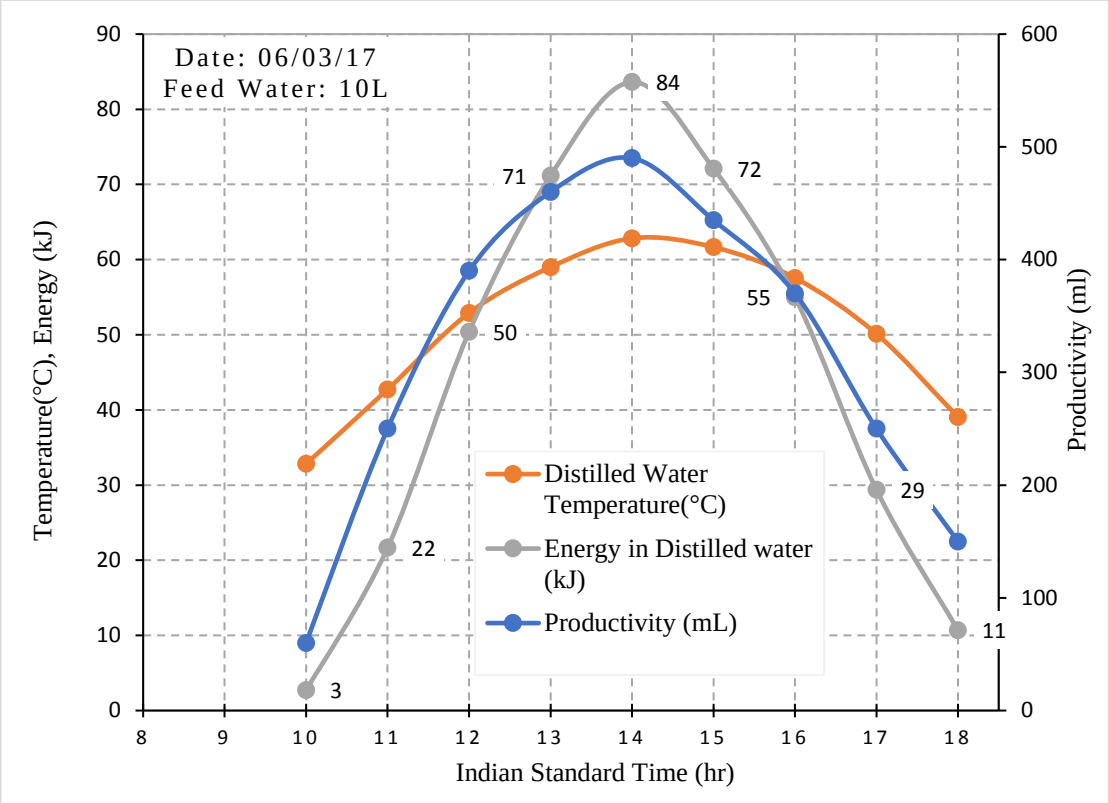

Figure 6.2(a): Hourly Energy Loss as Heat in Distilled Water on Date 06/03/17

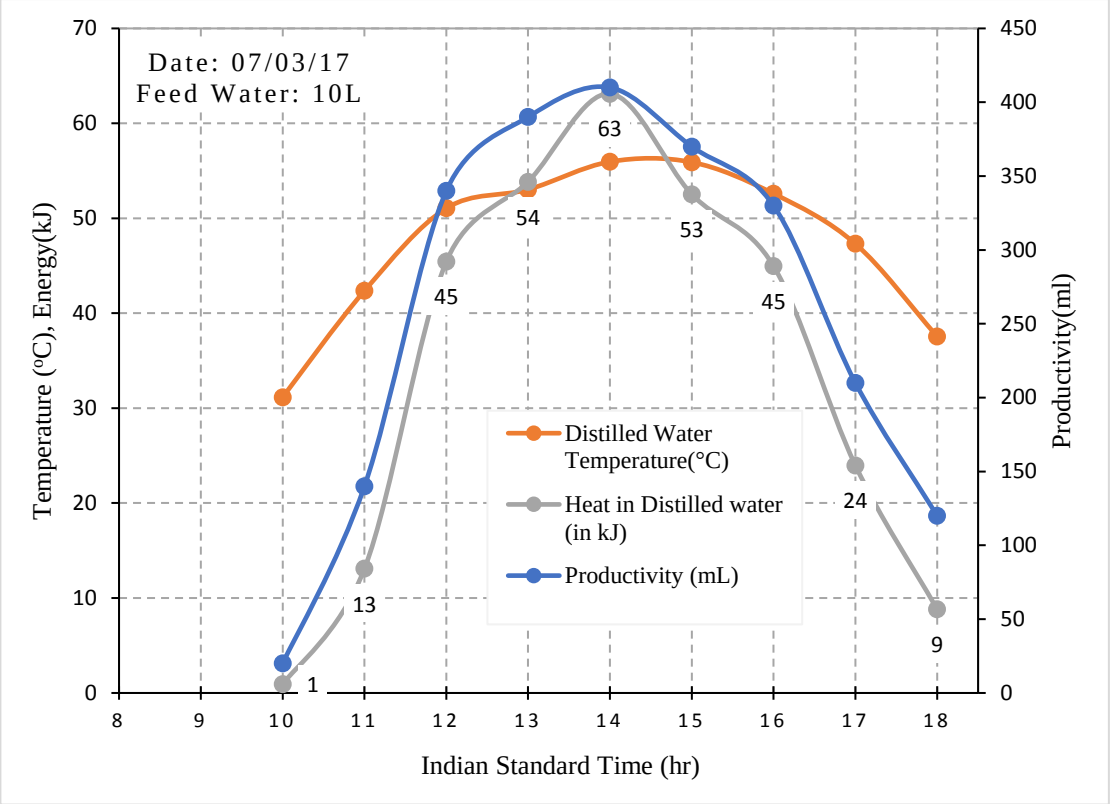

Figure 6.2(b): Hourly Energy Loss as Heat in Distilled Water on Date 07/03/17

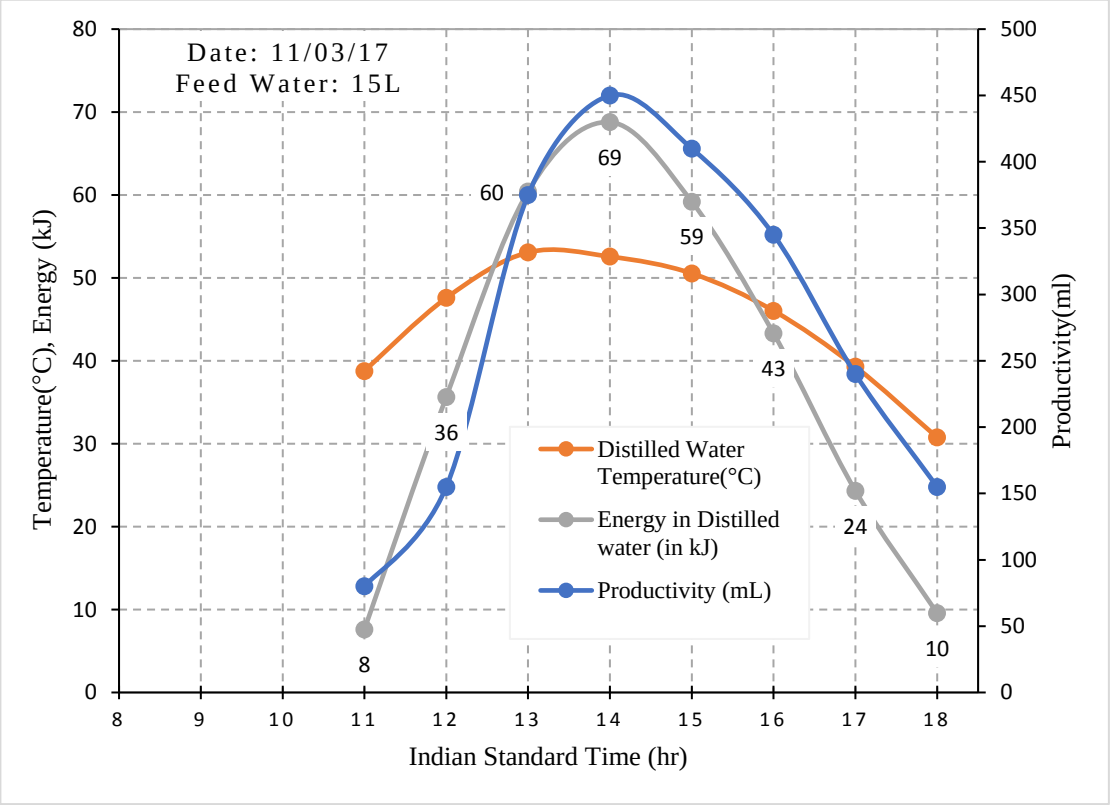

Figure 6.2(c): Hourly Energy Loss as Heat in Distilled Water on Date 11/03/17

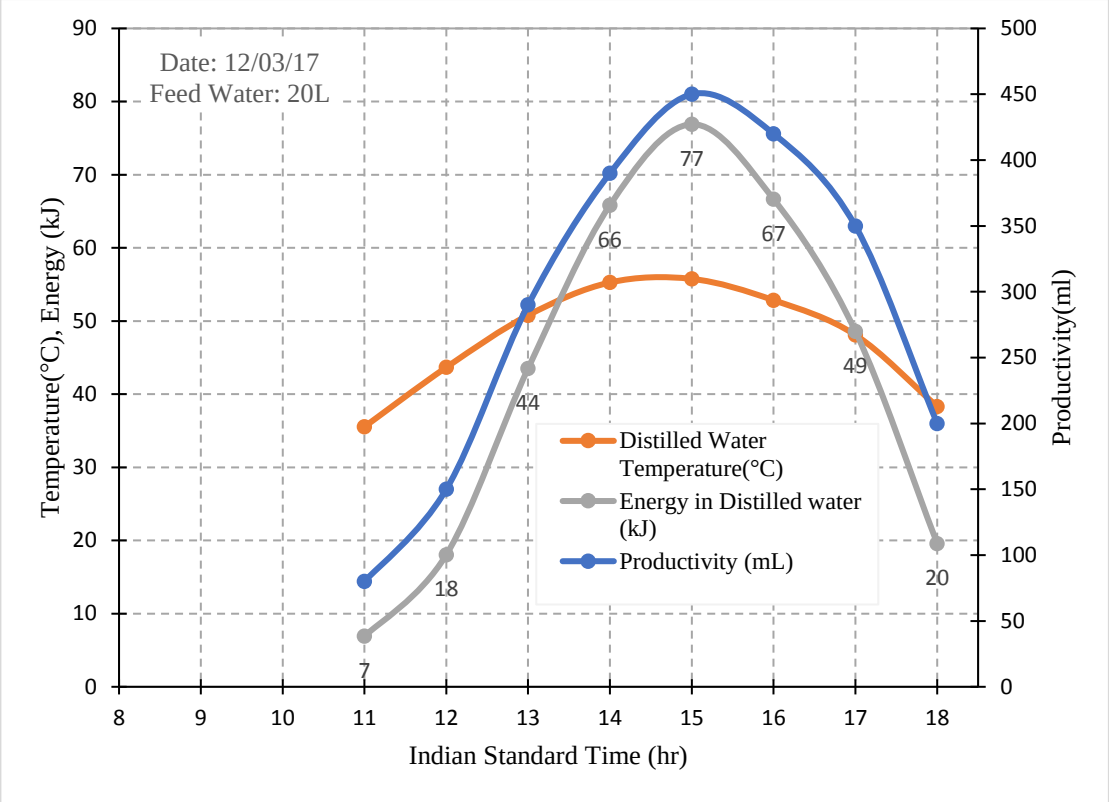

Figure 6.2(d): Hourly Energy Loss as Heat in Distilled Water on Date 12/03/17

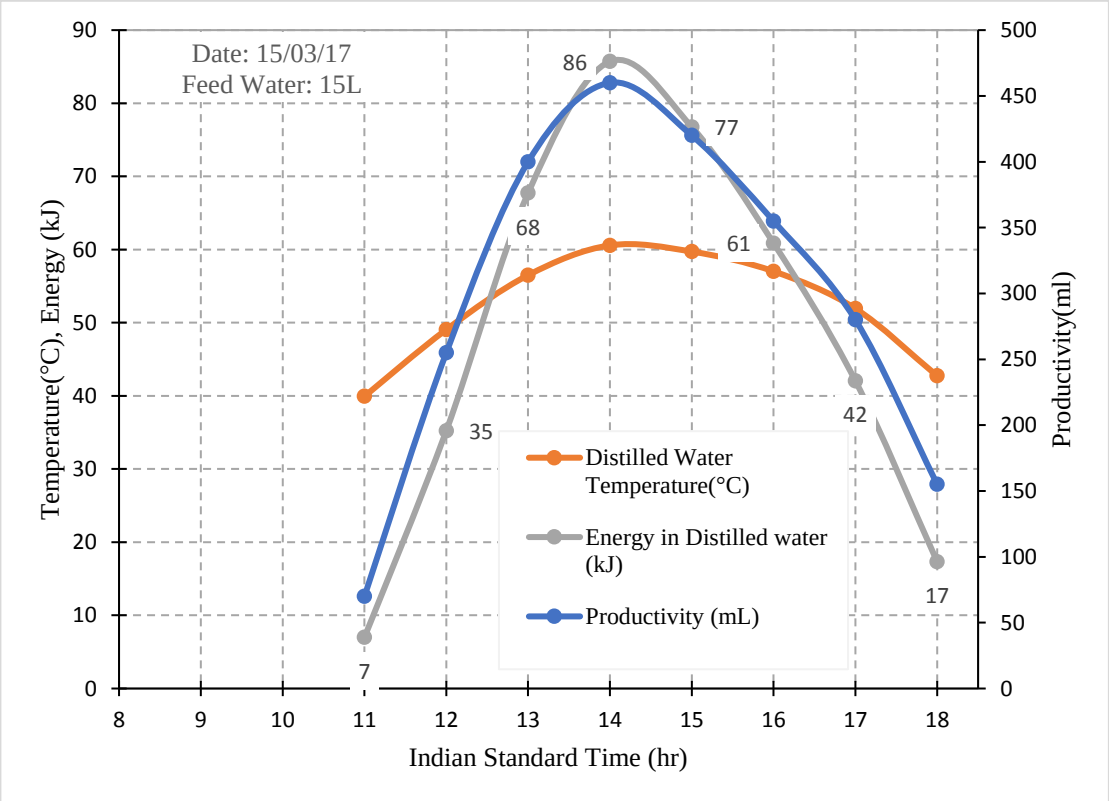

Figure 6.2(e): Hourly Energy Loss as Heat in Distilled Water on Date 15/03/17

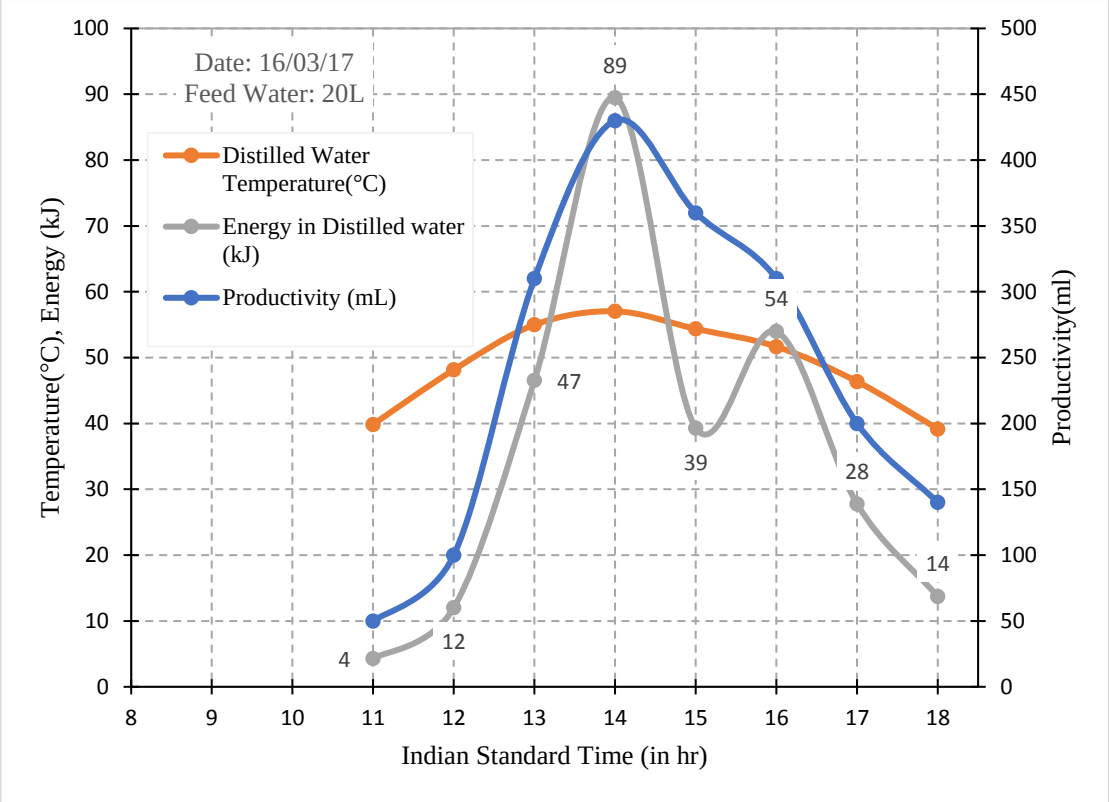

Figure 6.2(f): Hourly Energy Loss as Heat in Distilled Water on Date 16/03/17

Above six graphs, Fig. 6.2(a) – (f) have been plotted for the energy carried by the hot distilled water, distilled water output and its temperature with time (hours). During the early hours of the experiment there was no production of the distilled water. The start of production of distilled water also depends upon the amount of feed water, that can be seen clearly from the graphs, i.e. 10Ltrs feed water production of the distilled water began from 10 am, whereas for 15Ltrs and 20Ltrs feed water the production of the distilled water began from 11 am. This is because more heat is required (in the case of 15ltrs and 20ltrs feed water) to raise the temperature of the basin water, which is responsible for the evaporation of water. Theoretically, energy lost as heat content of distilled water should decreases with increase in the feed water quantity as distilled water production rate for 15Ltrs and 20Ltrs case is less than that of in 10Ltrs. Thus, the heat carried in distilled water is less in 15Ltrs and 20Ltrs cases. Total heat that carried by distilled water throughout the day is about 2 – 3% of the total solar energy that falls on the solar still.

6.3. Energy Lost as Leakage of Water Vapour

Some amount of water escapes from the solar still in the form of vapours from inlet and outlet pipes and gaps between the glass and the frame. It carries evaporative heat with it.

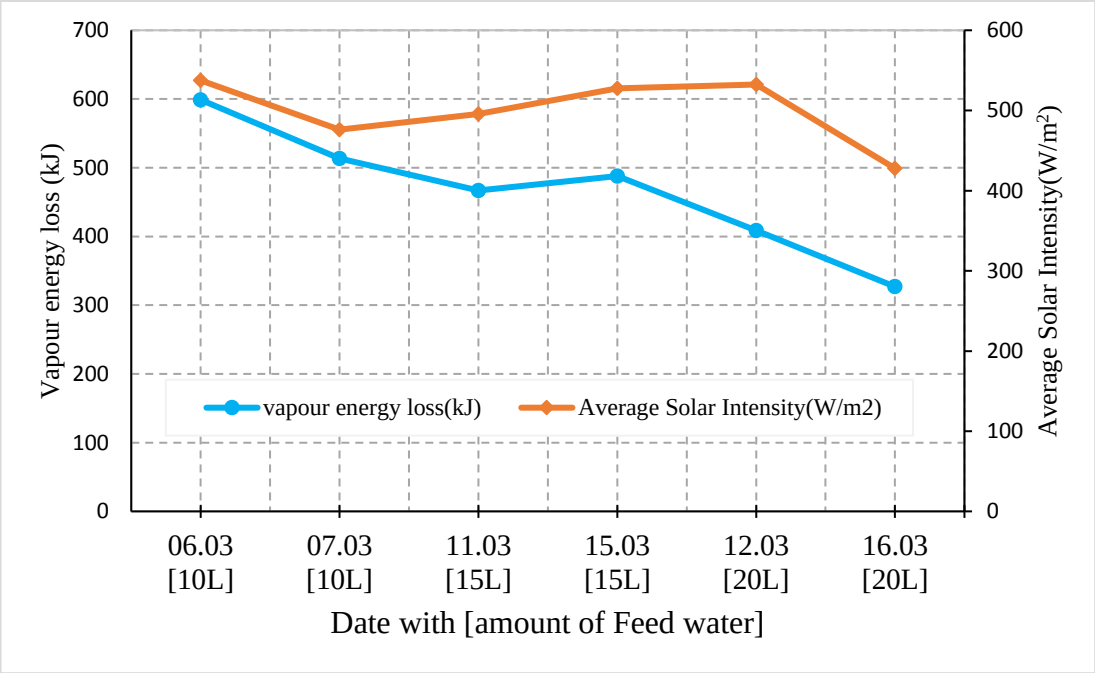

Figure 6.3(a): Varaition of Vapour Loss with Avg. Solar Intensity

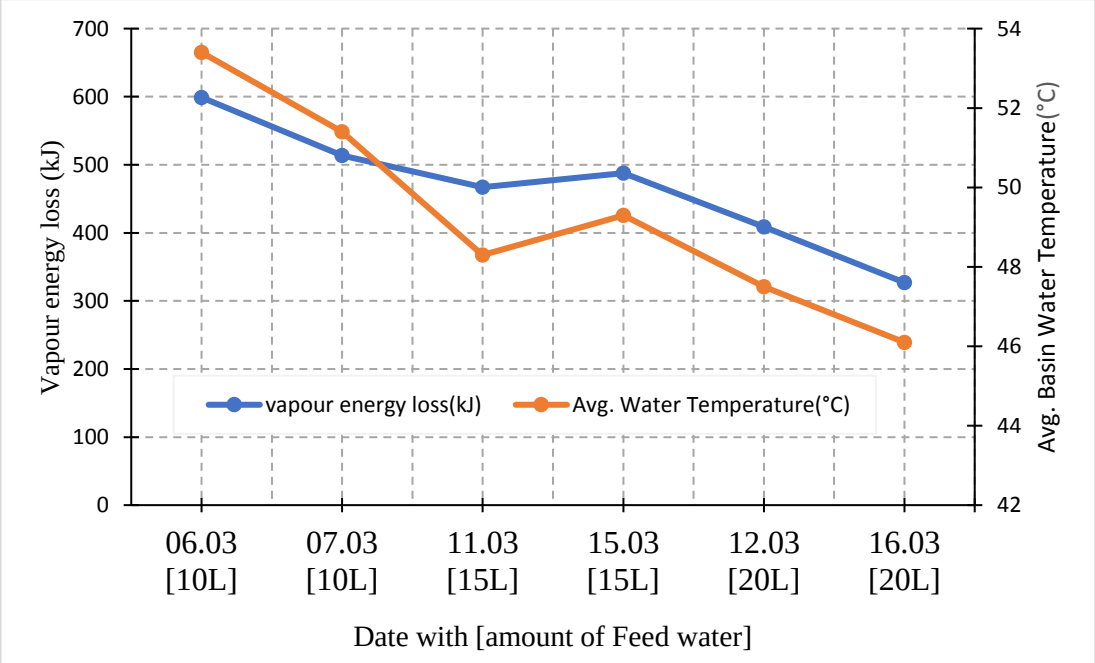

Figure 6.3(b): Varaition of Vapour Loss with Avg. Basin Water

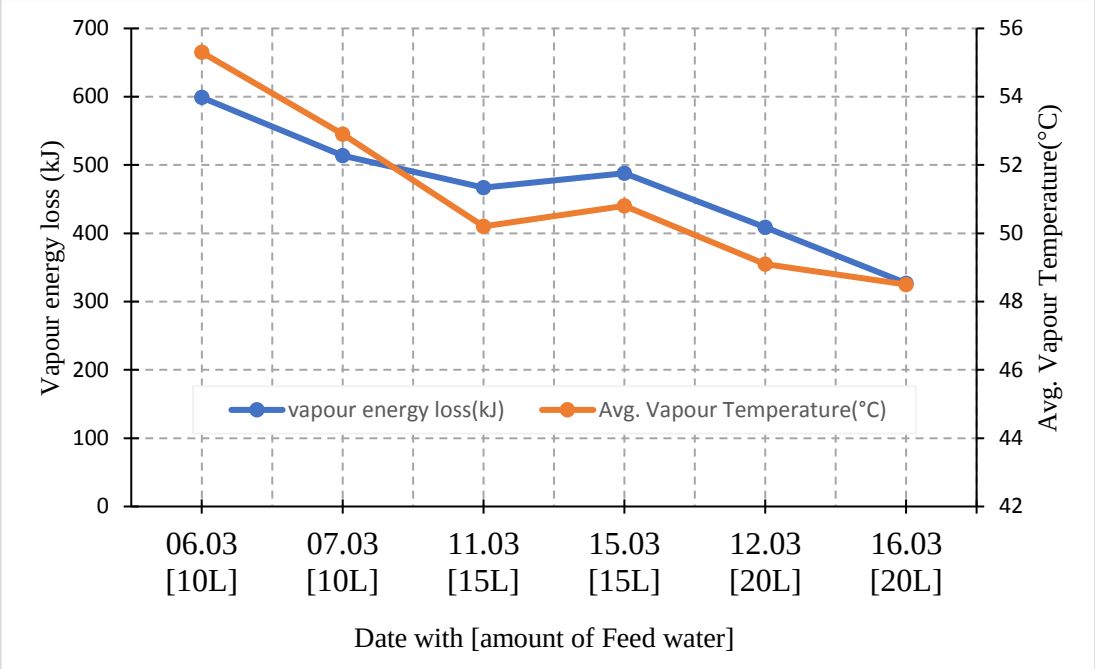

Figure 6.3(c): Varaition of Vapour Loss with Avg. Vapour Temperature

Above graphs, Fig. 6.3(a) – (c), have been plotted for energy lost as vapour in a whole day, for all six experimental days. The amount of vapour loss for 10Ltrs feed water was 265 ml and 220 ml on 6th and 7th Mar., respectively, for 15Ltrs feed water was 200 ml and 205 ml on 11th and 15th Mar., respectively and for 20Ltrs feed water was 175 ml and 140 ml on 12th and 16th Mar. respectively.

This shows a trend, i.e. as the amount of feed water increases, the amount vapour loss decreases. This is because of the temperature of basin water is lower for 20Ltrs than that for 15Ltrs feed and the temperature of basin water is for 15Ltrs feed water is lower from that for 10Ltrs feed water. The lower temperature leads to lower evaporation rate with low vapour pressure inside the solar still, and thus lower vapour losses. The vapour losses are more for 10Ltrs of feed water than that for 15Ltrs, and similarly, more for 15Ltrs than that for 20Ltrs of feed water. This trend is not observed always due to the variation in average solar intensity of the day, which leads to variation in feed water temperature. Energy lost as escaped water vapours is about 3% of the total energy that is incident of the solar still. This loss can be the minimized by sealing the inlet of the solar still by cork, and by dipping the outlet pipe in the jar filled with distilled water, and by improving the sealing between the glass cover and still walls.

6.4. Heat Balance

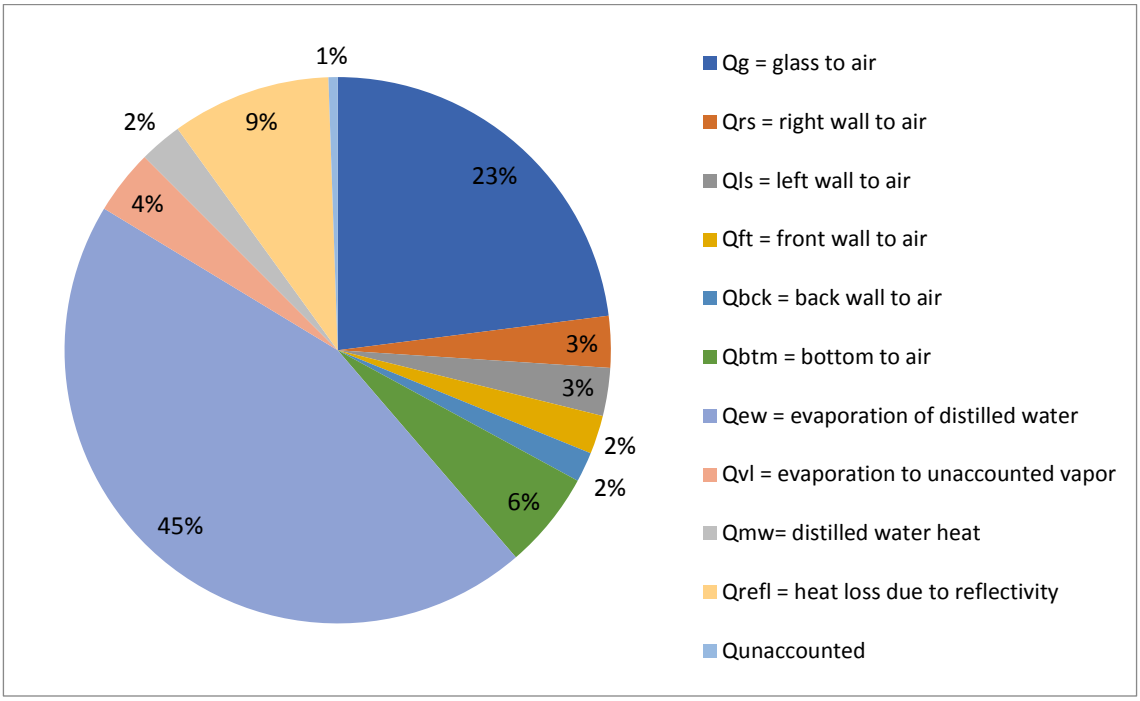

Figure 6.4(a): Average Heat Balancing for Whole Day on 06/03/17

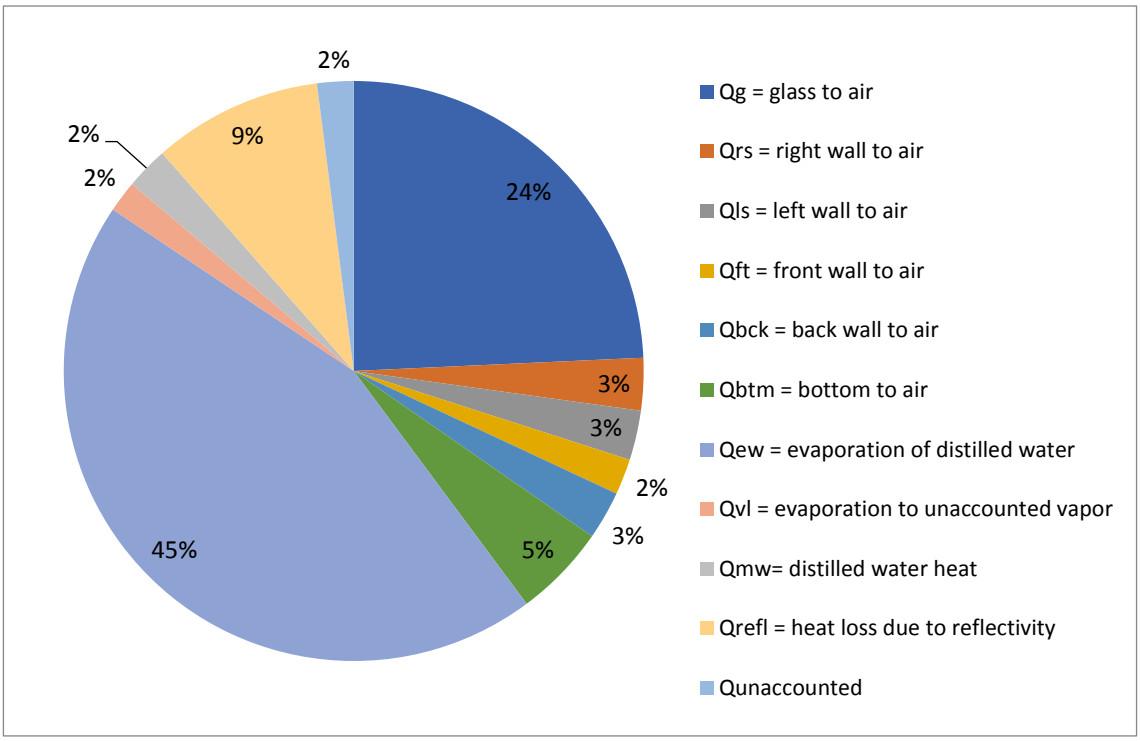

Figure 6.4(b): Average Heat Balancing for Whole Day on 07/03/17

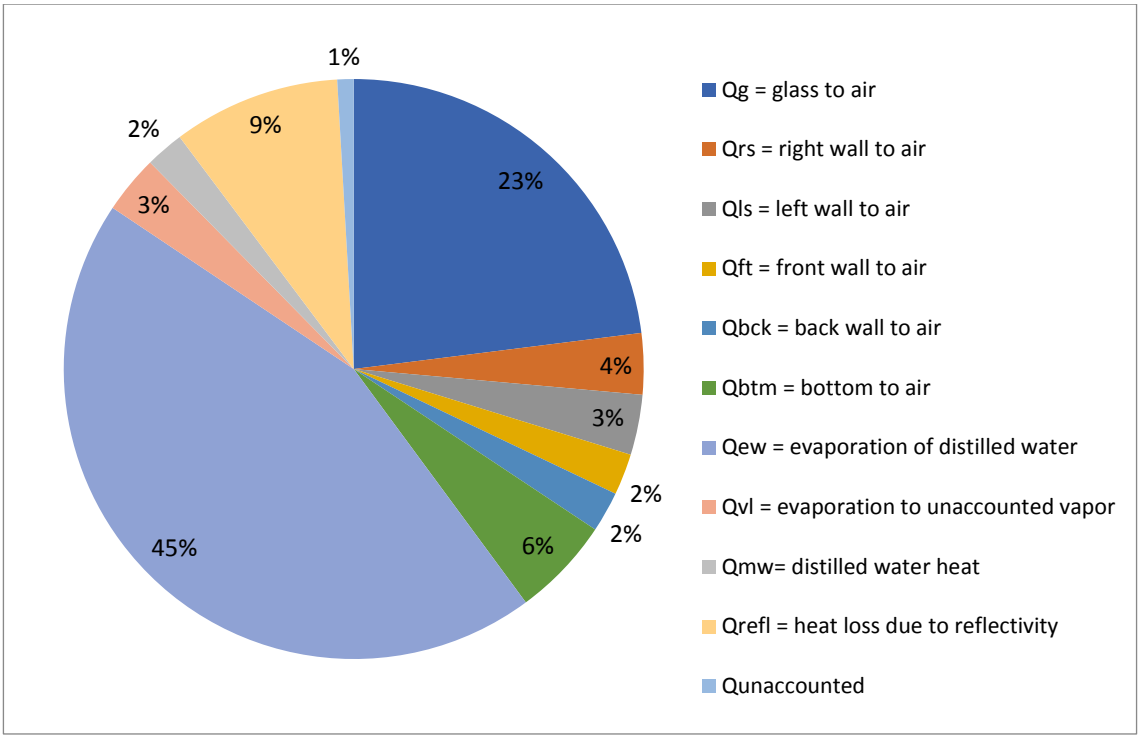

Figure 6.4(c): Average Heat Balancing for Whole Day on 11/03/17

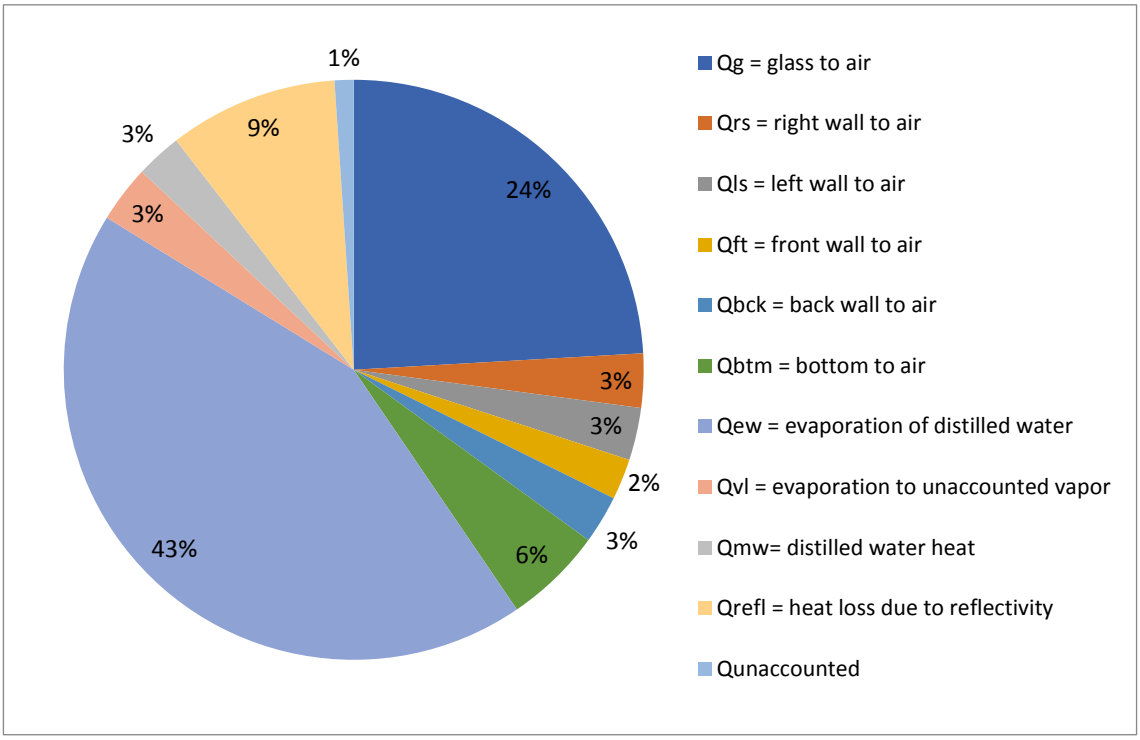

Figure 6.4(d): Average Heat Balancing for Whole Day on 15/03/17

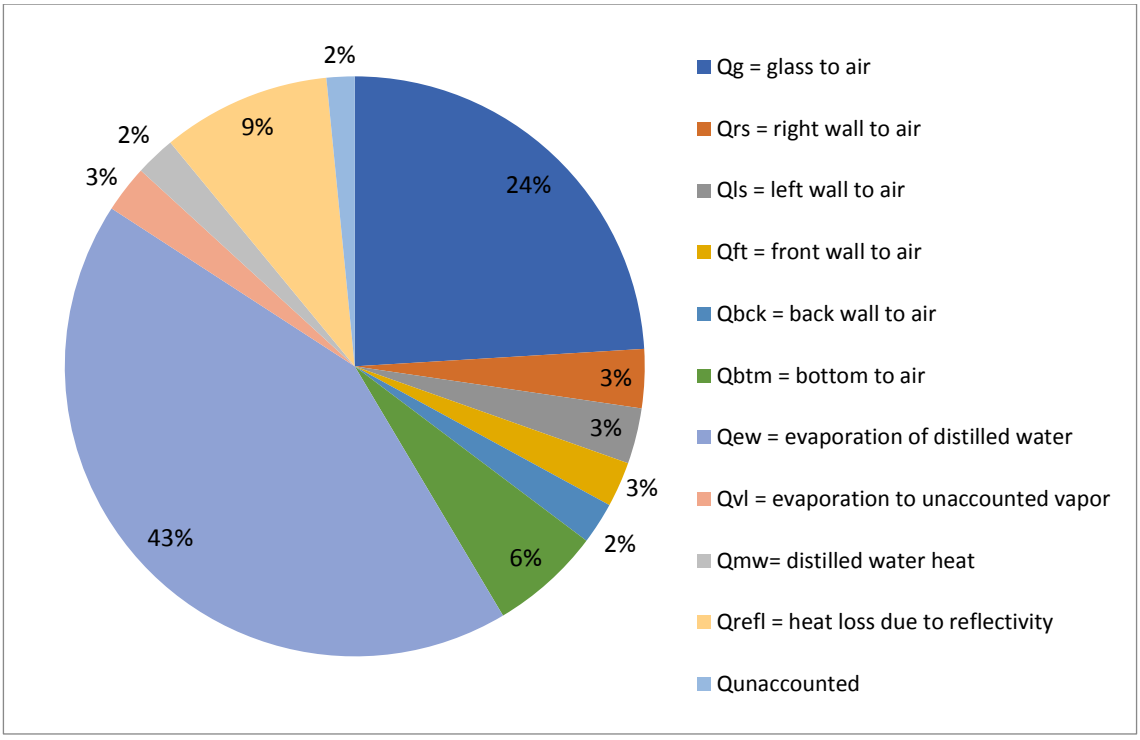

Figure 6.4(e): Average Heat Balancing for Whole Day on 12/03/17

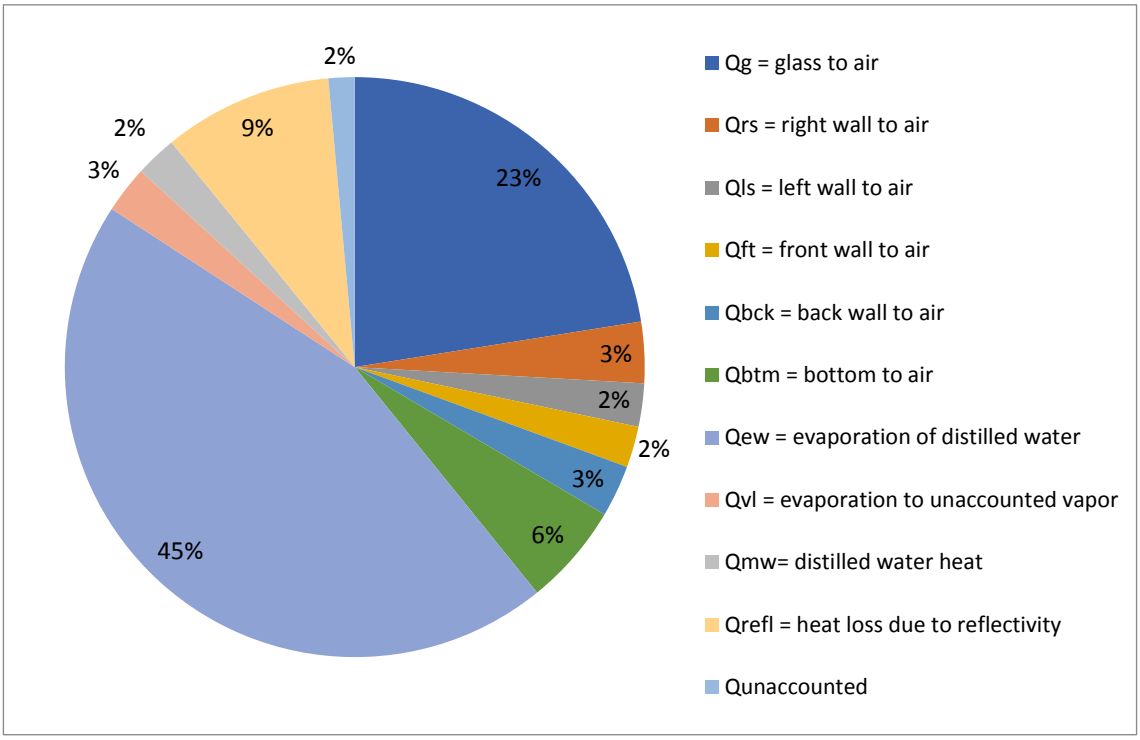

Figure 6.4(f): Average Heat Balancing for Whole Day on 16/03/17

Above six charts, Fig 6.4(a) to (f), show heat balance for the solar still. Various heat losses enumerated are - heat loss from glass to sky (23%), heat loss from right side, left side, front, back, and bottom wall (3%, 2%, 2%, 2%, 6% respectively), heat lost due to the evaporation of feed water and of unaccounted vapor loss (45% and 4% respectively), heat carried by the distilled water (3%), and losses due to the reflection of the solar radiation from inclined glass surface (9%). 1% of the solar energy input to the solar still is unaccounted for . Unaccountable heat may have been absorbed by the solar still or may be the error in the calculation of heat losses through the surfaces.

Table 6.1: Average Heat Balanced Sheet of Six Days

Date	Heat in (%)											
	Q_g	Q_{rs}	Q_{ls}	Q_{ft}	Q_{bck}	Q_{btm}	Q_{ew}	Q_{vl}	Q_{mw}	Q_{refl}	Q_{unacc}	Q_{in}
06.03.17	23	3.1	2.8	2.3	1.8	5.8	45	3.8	2.5	9.4	0.5	100
07.03.17	24	2.9	2.8	2.0	2.7	5.2	45	1.7	2.4	9.4	2.0	100
11.03.17	23	3.4	3.4	2.3	2.3	5.6	45	3.2	2.1	9.5	0.6	100
15.03.17	24	3.0	2.9	2.3	2.7	5.5	43	3.2	2.6	9.4	1.1	100
12.03.17	24	3.3	3.1	2.5	2.3	6.2	43	2.6	2.2	9.4	1.6	100
16.03.17	23	3.4	2.4	2.3	2.9	5.7	45	2.6	2.3	9.5	0.9	100
Average	**24**	**3.2**	**2.9**	**2.3**	**2.4**	**5.7**	**44**	**2.9**	**2.4**	**9.4**	**1.1**	**100**

Chapter 7.
Conclusions

In this study of heat and mass balance of the single slope solar still, ten sets of experiments were done from 6th to 16th March, 2017. These experiments were carried out with the variation in feed water quantity, i.e. 10L, 15L, and 20L. On the basis of clear sky or minimal variation in solar intensity, six set of the experimental data were selected, i.e. two sets of data for 10L, 15L, and 20L each. Following conclusions are drawn on the basis of observations and analysis.

- Vapour loss increases with the increase in average basin water temperature. This is because of the evaporation rate increases with the basin water temperature. Energy lost due to vapour loss account for 2 – 3% of the total energy that enters the solar still. The quantity of the vapour loss also decreases with the increase in the feed water quantity in the solar still because with the increase in feed water quantity, average temperature of the water in the basin decreases. These vapour loss can be minimized by improving the sealing between the glass cover and the still walls.
- Loss of incident Solar Radiations through reflection: Reflection of the solar radiation from the surface of the glass was of the order of 10% of the total energy that was incident on the solar still. The amount of reflection loss depends on the angle of the incidence radiation and solar intensity. These reflection losses can be minimized by using anti-reflective coated glass.
- Loss of energy as heat carried by the distilled water: Distilled water carries energy with it as the temperature of distilled water temperature is considerably higher than the temperature of the feed water. In this study, the feed water temperature was about 20 °C, whereas distilled water temperature goes up to 63 °C. Thus, energy loss due to heat content in distilled water for the whole day was about 2 – 3% of the total energy that was incident on the solar still.
- Surface heat losses which accounts 16 – 17% of total energy. Out of this bottom surface and front surface are found to be major source of heat loss per unit surface area, i.e. 6% from bottom (0.88 m^2) and 2 – 3% from the front (0.012m^2). This uneven heat loss from the front surface is coming out to be more

as the insulation is not present in the front wall. If insulation is provided this front surface, heat loss can be minimized.

7.1. Future Scope

- Distilled water output and temperature in the basin follows incident solar radiations closely. Thus, a mathematical model dependent on incident solar radiations and distilled water output predicting the performance of a solar still can be developed.
- The reflectivity of the glass cover can be minimized by using glass coated with anti-reflective coating. Further comparative experimental study of solar still with and without anti-reflective coated glass can be carried out.

References

Abdul-Wahab S.A., Al-Hatmi Y.Y., (2012), "Study of the Performance of the Inverted Solar Still Integrated with a Refrigeration Cycle", *Procedia Engineering*, 33, 424-434.

Abujazar M.S., Fatihaha S., Rakmi A.R., Shahrom M.Z., (2016), "The effects of design parameters on productivity performance of a solar still for seawater desalination: A review", *Desalination*, 385, 178–193.

Alaudeen A., Johnson K., Ganasundar P., Abuthahir A.S., Srithar K., (2015), "Study on stepped type basin in a solar still", *Journal of King Saud University – Engineering Sciences*, 27, 143-150.

Appadurai M., Velmurugan V., (2015), "Performance analysis of fin type solar still integrated with fin type mini solar pond", *Sustainable Energy Technologies and Assessments*, 9, 30-36.

Arunkumar T., Velraj R., Denkenberger D.C., Sathyamurthy R., Kumar K.V., Ahsan A., (2016), "Productivity enhancements of compound parabolic concentrator tubular solar stills", *Renewable Energy*, 88, 391-400.

Badran A.A., Al-Hallaq A.A., Eyal Salman I.A., Odat M.Z., (2005), "A solar still augmented with a flat-plate collector", *Desalination*, 172, 227-234.

Bhardwaj R., Kortenaar M.V., Mudde R.F., (2016), "Inflatable plastic solar still with passive condenser for single family use", *Desalination*, 398, 151-156.

Durkaieswaran P., Murugavel K.K., (2015), "Various special designs of single basin passive solar still – A review", *Renewable and Sustainable Energy Reviews*, 49, 1048–1060.

El-Samadony Y.A.F., El-Maghlany W.M., Kabeel A.E., (2016), "Influence of glass cover inclination angle on radiation heat transfer rate within stepped solar still", *Desalination*, 384, 68–77.

Patel N.S., Shah R.R., Patel N.M., Shah J.K., Bhatt S.B., (2013), "Effect of various parameters on different types of solar still: case study", *International Journal of Innovative Research in Science, Engineering and Technology*, 2, 1726-1731.

Panchal H.N., (2015), "Enhancement of distillate output of double basin solar still with vacuum tubes", *Journal of King Saud University – Engineering Sciences*, 27, 170-175.

Sharshir S.W., Peng G., Yang N., Eltawil M.A., Ahmed-Ali M.K., Kabeel A.E., (2016), "A hybrid desalination system using humidification-dehumidification and solar stills integrated with evacuated solar water heater", *Energy Conversion and Management*, 124, 287–296.

Velmurugan V., Pandiarajan S., Guruparan P., Subramanian L.H., Prabaharan C.D., Srithar K., (2009), "Integrated performance of stepped and single basin solar stills with mini solar pond", *Desalination*, 249, 902-909.

Rajaseenivasan T., Srithar K., (2015), "Performance investigation on solar still with circular and square fins in basin with CO2 mitigation and economic analysis", *Desalination*, 124, 89-97.

Pradeep S.G., Jain K., Varun N., Kumar V.V., (2015), "Solar powered water distillation with concave evaporation surface", *International Research Journal of Engineering and Technology*, 2, 2275-2279.

Kabeel A.E., Omara Z.M., Younes M.M., (2015), "Techniques used to improve the performance of the stepped solar still—A review", *Renewable and Sustainable Energy Reviews*, 46, 178–188.

Omara Z.M., Kabeel A.E., Younes M.M., (2014), "Enhancing the stepped solar still performance using internal and external reflectors", *Energy Conversion and Management*, 78, 876–881.

Kabeel A.E., Omara Z.M., Younes M.M., (2013), "Enhancing the stepped solar still performance using internal reflectors", *Desalination*, 314, 67–72.

Raju V.R., Narayana R.L., (2016), "Effect of flat plate collectors in series on performance of active solar still for Indian coastal climatic condition", *Journal of King Saud University – Engineering Sciences*, 37, 231–239.

Rajaseenivasan T., Srithar K., (2016), "Performance investigation on solar still with circular and square fins in basin with CO2 mitigation and economic analysis", *Desalination*, 380, 66–74.

Setoodeh N., Rahimi R., Ameri A., (2011), "Modeling and determination of heat transfer coefficient in a basin solar still using CFD", *Desalination*, 268, 103–110.

Rahbar N., Esfahani J.A., (2013), "Productivity estimation of a single-slope solar still: Theoretical and numerical analysis", *Energy*, 49, 289-297.

Hamadou O.A., Abdellatif K., (2014), "Modeling an active solar still for sea water desalination process optimization", *Desalination*, 354, 1–8.

Shatat M.I.M., Mahkamov K., (2010), "Determination of rational design parameters of a multi-stage solar water desalination still using transient mathematical modeling", *Renewable Energy*, 35, 52–61.

Sharshir S.W., Yang N., Peng G., Kabeel A.E., (2016), "Factors affecting solar stills productivity and improvement techniques: a detailed review", *Applied Thermal Engineering*, 47, 1-35.

Raut H.K., V.A., Nairb A.S., Ramakrishna S., (2011), "Anti-reflective coatings: A critical, in-depth review", *Energy and Environment Science*, 4, 3779-3804.

Swatowsk B., Stapinski T., Drabczyk K., Panek P., (2011), "The role of anti-reflective coatings in silicon solar cells– the influence on their electrical parameters", *Optica Applicata*, 41, 487-492.

Thosar A.J., Thosar M., Khanna R.K., (2014), "Optimization of Anti-Reflection Coating for Improving the Performance of GaAs Solar Cell", *Indian Journal of Science and Technology*, 7, 637–641.

Omara Z.M., Kabeel A.E., Younes M.M., (2013), "Desalination of the brackish water using a passive solar still with a heat energy storage system", *Desalination*, 324, 10-20.

Rufuss D. D., Iniyan S., Suganthi L., Davies P.A., (2016), "Solar stills: A comprehensive review of designs, performance and material advances", *Renewable and Sustainable Energy Reviews*, 63, 464–496.

Publication

- Ankur Agrawal, Gautam Saini, Nirupam Rohatgi, (2017), "A Heat and Mass Balance Study of a Solar Still Investigating Ways to Improve its Performance", *International Journal of Innovative Research in Science, Engineering and Technology*, 6, 10592-10601.

Appendix

Properties/parameters of material used in the experimental analysis are given below:

1) Area of different surfaces:

S. No.	Surface	Area (m^2)
1	Side Walls	0.2907
2	Front surface	0.012
3	Bottom surface	0.88
4	Back surface	0.5716
5	Glass surface	0.8088

2) Properties of Water:

- Prandtl No., Pr = 0.71
- Kinematic viscosity, $\nu = 16.9 \times 10^{-6}$ m^2/s
- Thermal conductivity, k = 0.027 W/mK
- Enthalpy of evaporation, h_{fg} = 2335 kJ/kg

3) Properties of different materials used:

Materials	Properties		
	Thickness (mm)	Thermal conductivity (W/m.K)	Emissivity (ε)
GI Sheet	0.5	18	0.88
Glass	5	0.80	0.97
Thermocol	25.4	0.036	-
Water	-	0.027	0.95